

CHAPTER II: Supplementary information

SYNTHESIS, ENZYME ASSAYS AND MOLECULAR DOCKING STUDIES OF FLUORINATED BIOISOSTERES OF SANTACRUZAMATE A AS POTENTIAL HDAC TRACERS

Muneer Ahamed^{1*}, **Koen Vermeulen**^{2*}, Michaël Schnekenburger³, Lise Román Moltzau^{4,9}, Finn Olav Levy^{4,9}, János Marton⁸, Mathy Froeyen⁵, Dag Erlend Olberg⁶, Marc Diederich^{3,7} and Guy Bormans²

¹ Centre for Advanced Imaging, University of Queensland, Brisbane, Australia

² Laboratory for Radiopharmaceutical Research, Department of Pharmaceutical and Pharmacological Sciences, KU Leuven, Leuven, Belgium

³ Laboratoire de Biologie Moléculaire et Cellulaire du Cancer, Hôpital Kirchberg, 9, rue Edward Steichen, L-2540 Luxembourg, Luxembourg

⁴ Department of Pharmacology, Institute of Clinical Medicine, University of Oslo and Oslo University Hospital, Oslo, Norway

⁵ Laboratory for Medicinal Chemistry, Rega Institute of Medical Research, KU Leuven, Leuven, Belgium

⁶ School of Pharmacy, University of Oslo and Norwegian Medical Cyclotron Centre, Oslo, Norway

⁷ Department of Pharmacy, Research Institute of Pharmaceutical Sciences, College of Pharmacy, Seoul National University, Seoul, Republic of Korea and Tumor Microenvironment Global Core Research Center, College of Pharmacy, Seoul National University, Seoul 151-742, South Korea

⁸ ABX advanced biochemical compounds, Biomedizinische Forschungsreagenzien GmbH, Radeberg, Germany

⁹ Center for Heart Failure Research, Faculty of Medicine, University of Oslo, Oslo, Norway

*These authors contributed equally to this work.

ORGANIC SYNTHESIS

General methods

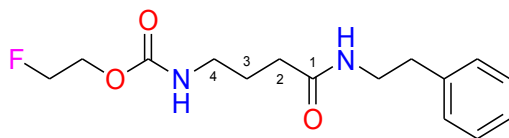
Reagents and solvents were purchased from major commercial suppliers and were used without further purification. Melting points were measured with a Büchi-535 instrument and the data are uncorrected. Column chromatography was performed on Kieselgel 60 Merck 1.09385 (0.040-0.063 mm). TLC was accomplished on Macherey-Nagel Alugram[®] Sil G/UV₂₅₄ 40x80 mm aluminum sheets [0.25 mm silica gel with fluorescent indicator] with the following eluent systems (each v/v): [A]: dichloromethane-methanol 9:1, [B]: ethyl acetate-methanol 8:2, [C]: ethyl acetate-chloroform 7:3, [D]: chloroform-methanol 9:1, [E]: ethyl acetate-hexane 8:2. The spots were visualized with a 254 nm UV lamp or with 5% phosphomolybdic acid in ethanol.

¹H-, ¹³C- and ¹⁹F-NMR spectra were obtained with a Bruker AV 500 (Avance 500 MHz) spectrometer at 298 K, using BBO probehead. For ¹H- and ¹⁹F-NMR experiments 10 mg of the appropriate derivative was dissolved in 500 µL of the corresponding deuterated solvent (CDCl₃ and CD₃OD). For measuring ¹³C-NMR- and 2D-spectra: 20 mg of the synthesized compound was dissolved in 500 µL solvent. Chemical shifts (δ) are in parts per million (ppm), and coupling constants (*J*) reported in Hertz. ¹H and ¹³C-NMR chemical shifts were referenced to the residual peak of CDCl₃ at 7.26 and 77.16 ppm, for proton and carbon respectively (CD₃OD: 3.31 and 49.00 ppm). Observation frequency: 500.130 MHz (¹H-NMR), 125.758 MHz (¹³C-NMR), and 470.592 MHz (for ¹⁹F-NMR spectra).

Homonuclear ¹H-¹H-COSY (Bruker Pulprog cosygpqf): observation frequency: 500.130 Mz, AQ = 0.239 sec, spectral width = 4280.82 Hz, D1 = 1.4 sec, NS = 16, DS = 8. Long-range ¹H-¹³C correlations (HMBC) spectra (Bruker Pulprog hmbcgpndqf): observation frequency: 500.130 MHz (¹H), 125.758 MHz (¹³C), AQ = 0.526 sec, spectral width = 7.78 ppm (f1), and 220 ppm (f2); D1 = 1.28 sec, NS = 32, DS = 16.

NMR Analysis

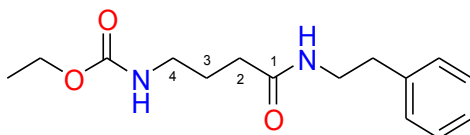
Table S1-A. NMR Data for Fluoroethyl-Santacruzamate A (**9**) in CDCl₃



| Position | δ_{H} mult. (J in Hz) | δ_{C} mult . | COSY | HMBC |
|-----------------------------------|-------------------------------------|--|--|--|
| 1 | - | 172.4 | - | |
| 2 | 2.17 t (7.0) | 33.6 | 3 | C-1, C-3, C-4 |
| 3 | 1.80 pent, (6.9) | 25.8 | 2, 4 | C-1, C-2, C-4 |
| 4 | 3.18 q (6.4) | 40.3 | 3, COONHCH ₂ | C-3, C-2, COONHCH ₂ |
| PhCH ₂ CH ₂ | 2.81 t (7.0) | 35.6 | PhCH ₂ CH ₂ | PhCH ₂ CH ₂ , Ph-C1, Ph-C2,6 |
| PhCH ₂ CH ₂ | 3.51 dd, (7.0 and 13.0) | 40.5 | PhCH ₂ CH ₂ , CONHCH ₂ | C-1, Ph-C1, PhCH ₂ CH ₂ |
| PhCH ₂ CH ₂ | 7.17-7.31 m | - | - | - |
| Ph-C1 | | 138.8 | - | PhCH ₂ CH ₂ , PhCH ₂ CH ₂ |
| Ph-C2,6 | | 128.6 | | PhCH ₂ CH ₂ |
| Ph-C3,5 | | 128.7 | | |
| Ph-C4 | | 126.4 | | |
| CONHCH ₂ | 5.89 br s | - | PhCH ₂ CH ₂ | |
| OCNHCH ₂ | 5.21 br s | - | 4 | |
| OCNHCH ₂ | - | 156.4 | - | |
| CH ₂ CH ₂ F | 4.21–4.31 m | 63.7 d (² J _{C,F} = 20.1) | CH ₂ CH ₂ F | CH ₂ CH ₂ F, FCH ₂ CH ₂ OOCNH |
| CH ₂ CH ₂ F | 4.50–4.61 m | 81.8 d (¹ J _{C,F} = 169.5) | CH ₂ CH ₂ F | CH ₂ CH ₂ F |

Table S1-B. Heteronuclear multiple bond correlations of Fluoroethyl-Santacruzamate-A (9)

| | | HMBC | | | |
|-----------------------------------|--------------------------|-----------------------------------|--|----------|--|
| Position | $\delta^1\text{H}$ [ppm] | C-1 | C-3 | C-4 | |
| 2-CH ₂ | 2.17 t | | | | |
| $\delta^{13}\text{C}$ [ppm] | | 172.4 | 25.8 | 40.3 | |
| Distance [bond] | | 2 | 2 | 3 | |
| | | | | | |
| Position | $\delta^1\text{H}$ [ppm] | C-1 | C-2 | C-4 | |
| 3-CH ₂ | 1.80 pent | | | | |
| $\delta^{13}\text{C}$ [ppm] | | 145.3 | 137.1 | 128.5 | |
| Distance [bond] | | 3 | 2 | 2 | |
| | | | | | |
| Position | $\delta^1\text{H}$ [ppm] | C-3 | C-2 | COONH | |
| 4-CH ₂ | 3.18 q | | | | |
| $\delta^{13}\text{C}$ [ppm] | | 25.8 | 33.6 | 156.4 | |
| Distance [bond] | | 2 | 3 | 3 | |
| | | | | | |
| Position | $\delta^1\text{H}$ [ppm] | PhCH ₂ CH ₂ | Ph-C-1 | Ph-C-2,6 | |
| PhCH ₂ CH ₂ | 2.81 t | | | | |
| $\delta^{13}\text{C}$ [ppm] | | 40.5 | 138.8 | 128.6 | |
| Distance [bond] | | 2 | 2 | 3 | |
| | | | | | |
| Position | $\delta^1\text{H}$ [ppm] | PhCH ₂ CH ₂ | Ph-C-1 | C-1 | |
| PhCH ₂ CH ₂ | 3.51 dd | | | | |
| $\delta^{13}\text{C}$ [ppm] | | 35.6 | 138.8 | 172.4 | |
| Distance [bond] | | 2 | 3 | 3 | |
| | | | | | |
| Position | $\delta^1\text{H}$ [ppm] | CH ₂ CH ₂ F | FCH ₂ CH ₂ OOCNH | | |
| CH ₂ CH ₂ F | 4.21-4.31 | | | | |
| $\delta^{13}\text{C}$ [ppm] | | 81.8 | 156.4 | | |
| Distance [bond] | | 2 | 3 | | |
| | | | | | |
| Position | $\delta^1\text{H}$ [ppm] | CH ₂ CH ₂ F | | | |
| CH ₂ CH ₂ F | 4.50-4.61 | | | | |
| $\delta^{13}\text{C}$ [ppm] | | 63.7 | | | |
| Distance [bond] | | 2 | | | |
| | | | | | |

Table S1-C NMR Data for Santacruzamate A (**6**, CAS RN: 1477949-42-0) in CDCl₃

| Position | 1. ABX* | | Pavlik et al. <i>J. Nat. Prod.</i> 2013 , 76, 2026-2033. | | 2. Leuven** | |
|------------------------------------|-------------------------------------|---------------------|---|---------------------|-------------------------------------|---------------------|
| | δ_{H} mult. (J in Hz) | δ_{C} | δ_{H} mult. (J in Hz) | δ_{C} | δ_{H} mult. (J in Hz) | δ_{C} |
| 1 | - | 172.5 | - | 172.5 | - | 172.7 |
| 2 | 2.16 t (7.0) | 33.6 | 2.17 (6.9) | 33.7 | 2.17 t (7.0) | 33.8 |
| 3 | 1.79 pent, (6.8) | 26.1 | 1.80 pent (6.8) | 26.1 | 1.78-1.83 m | 26.3 |
| 4 | 3.16 q (6.1) | 40.1 | 3.18 q (5.9) | 40.2 | 3.17 t (6.2) | 40.3 |
| PhCH ₂ CH ₂ | 2.82 t (7.1) | 35.6 | 2.83 t (6.8) | 35.7 | 2.82 t (7.0) | 35.8 |
| PhCH ₂ CH ₂ | 3.51 dd, (7.0 and 13.0) | 40.6 | 3.53 q (6.8) | 40.6 | 3.51 q (6.2) | 40.8 |
| PhCH ₂ CH ₂ | 7.18-7.31 m | - | 7.22-7.30 m | - | 7.18-7.32 | - |
| Ph-C1 | | 138.8 | | 138.9 | | 139.1 |
| Ph-C2,6 | | 128.6 | | 128.6 | | 128.9 |
| Ph-C3,5 | | 128.7 | | 128.8 | | 128.8 |
| Ph-C4 | | 126.4 | | 126.5 | | 126.6 |
| CONHCH ₂ | 5.93 br s | - | 5.92 br s | - | 6.02 br s | - |
| OCNHCH ₂ | 4.93 br s | - | 4.92 br s | - | 5.0 br s | - |
| OCNHCH ₂ | - | 157.1 | - | 157.1 | - | 157.3 |
| COOCH ₂ CH ₃ | 4.08 q (7.1) | 60.8 | 4.1 q (6.9) | 60.8 | 4.10 (7.0) | 60.9 |
| COOCH ₂ CH ₃ | 1.22 t (7.1) | 14.6 | 1.23 t (7.3) | 14.7 | 1.23 t (7.1) | 14.8 |

Colourless Powder, mp. 114-115 °C, Lit. [Pavlik et al. 2013] mp. 112-113 °C.

HRMS (ESI) Calcd. For C₁₅H₂₃N₂O₃ [M+H]⁺: 279.1703. Found: 279.1846.

*500 MHz, CDCl₃ [Data not shown]

**400 MHz CDCl₃ [Figure S10 and Figure S11]

Hydrogen bonding contacts

Table S2 Predicted H-bond interactions, with the distance between the corresponding heteroatoms in Å, π - π interactions, distance of Zn²⁺ atom with the carbonyl oxygen (unless otherwise stated) for compounds 1-8. H-bonding and hydrophobic interactions are predicted by poseview or Ligplot analysis.

| <i>Cpd</i> | <i>Hydrogen Bonds (Heteroatom distance Å)</i> | <i>π-π interaction (Distance in Å)</i> | <i>Distance of Zn²⁺ in Å</i> | <i>Hydrophobic interactions</i> |
|------------|--|--|---|--|
| 1 | O-His145A (2.72) NH-His146A (2.76) O-Tyr308A (2.58) H-His183A (2.75) O-Tyr209A (2.90) | Tyr209A (3.36) | 1.79 (OH) 2.06 (CO) | Phe155A Phe210A His183A Leu276A Tyr209A |
| 2 | O-His145A (3.50) O-His146A (3.24) NH-Tyr308A (2.73) O-Asp181A (2.50) NH-Asp104A (2.58) | Phe155A (3.47) Phe210A (4.04) | 1.78 (CO) 4.23 (OH) | Asp186A Glu151A Phe210A Phe155A Lys149A |
| 3 | OH-His145A (3.14) OH-Gly143A (3.48) NH-Gly154A (3.14) | Phe155A (3.14) Phe210A (3.57) | 1.72 (CO) 3.79 (OH) | Phe210A Asp104 Phe155A Gly154A |
| 4 | O-His145A (3.48) O-His146A (3.20) O-Asp181A (3.32) NH-Tyr308A (3.59) | Phe155A (2.89) Phe210A (3.30) | 1.75 (CO) 3.54 (OH) | Phe155A Asp104A Leu276A Pro34A |
| 5 | CO-His145A (3.92) NH-His146A (3.35) | None | 1.80 (CO) | Ser153A Phe210A Gly154A Asp104A His210A Pro106A |
| 6 | CO-His145A (2.58) NH-His146A (2.73) O-Tyr308A (2.66) H-His183A (2.87) | None | 1.96 (CO) 1.91 (OH) | Leu276A Phe210A |
| 7 | O-His145A (3.76) | Phe155A (3.72) | 1.90 (OMe) | Phe210A His183A His146A |
| 8 | NH-Gly154A (2.73) NMe ₂ -Glu103A (2.90) NMe ₂ -Asp104A(2.71) | None | 2.39 (CO) | Phe155A Phe210A His33A His146A Leu276A |

Pan-HDAC and HDAC2 inhibition assays

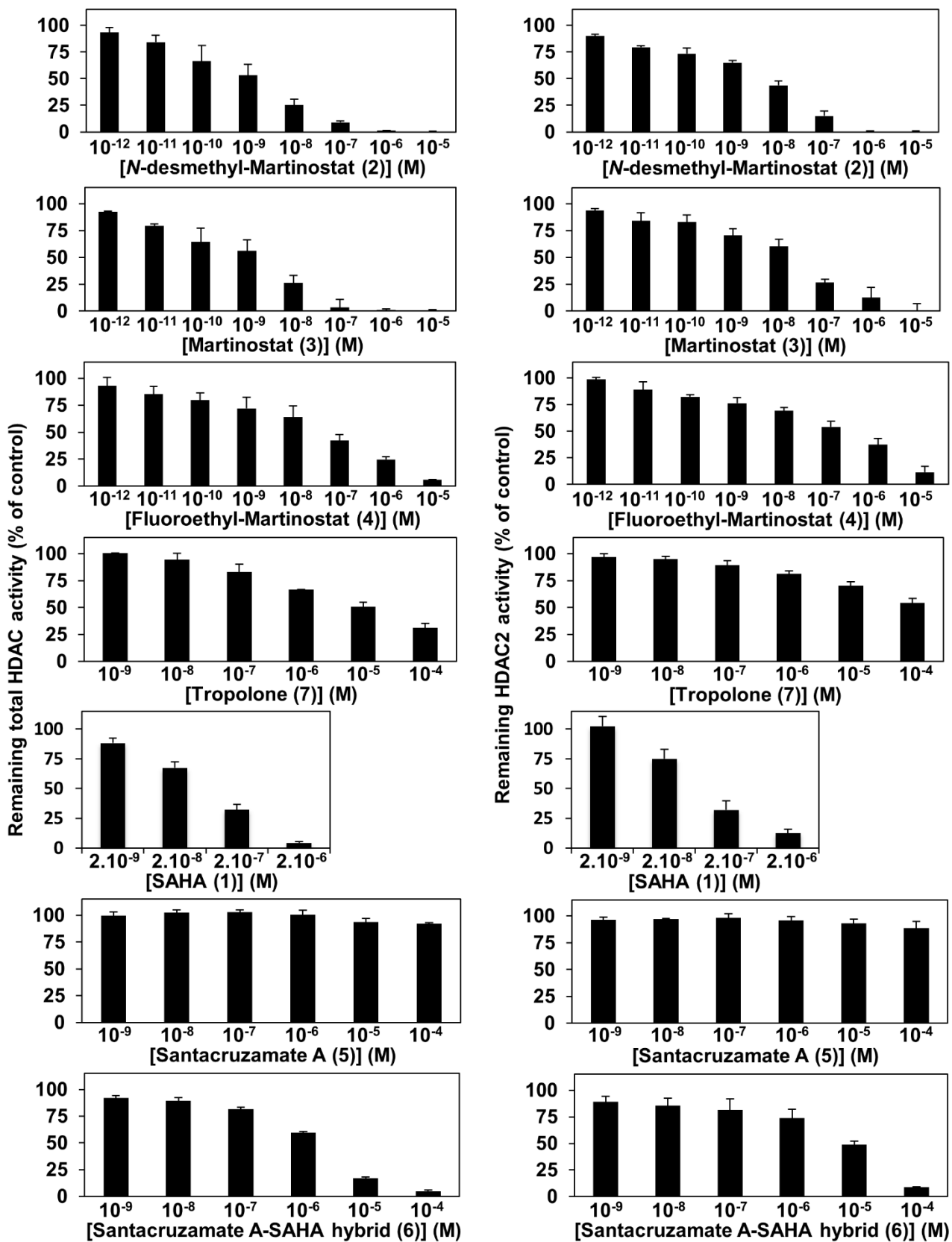


Figure S1 Effect of compounds 1-7 on total HDAC or HDAC2 activities between 1 nM and 100 μ M.

NMR spectral data for all final compounds

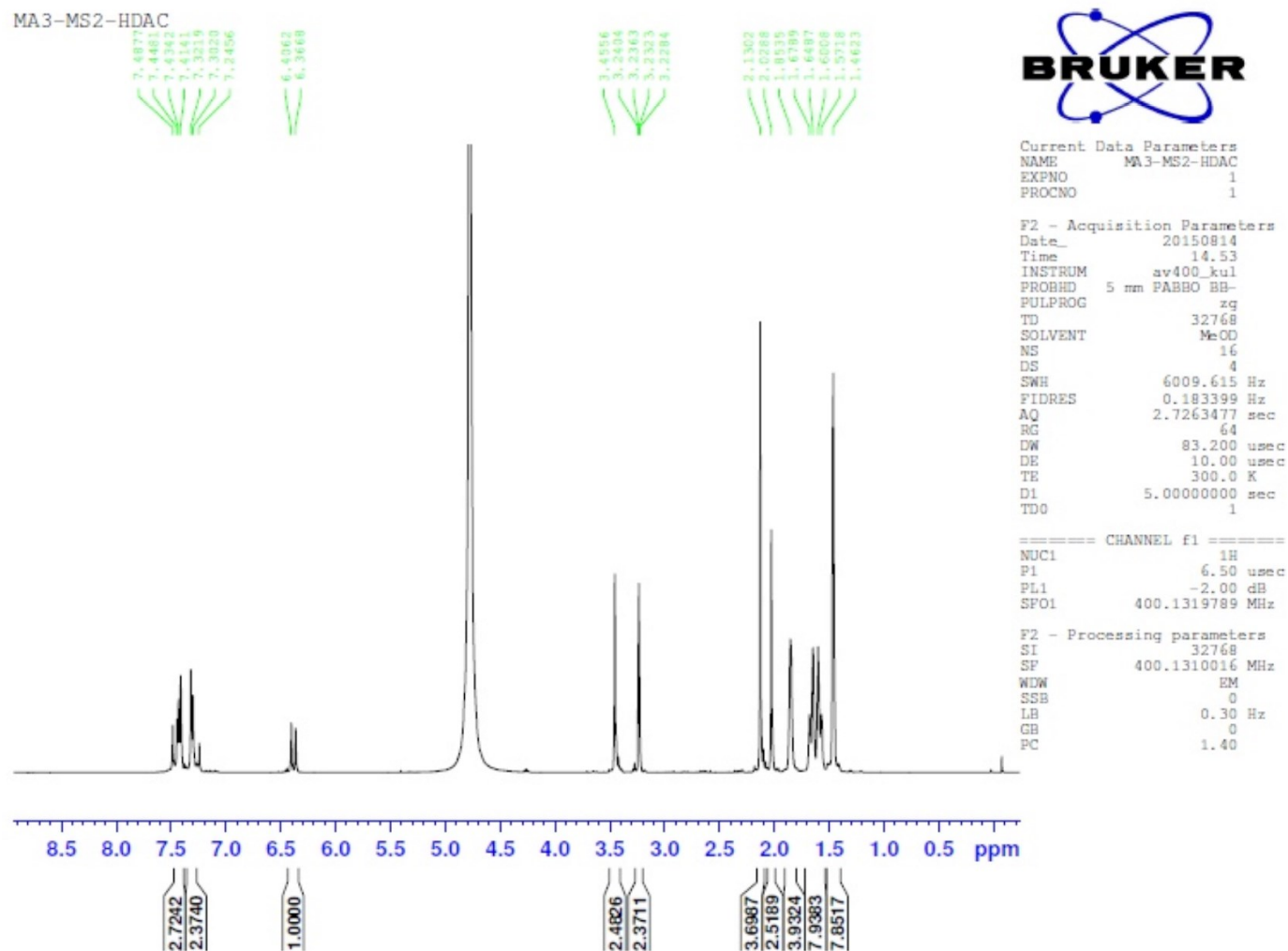


Figure S2: ¹H-NMR spectrum of martinostat (**3**) in CD₃OD.

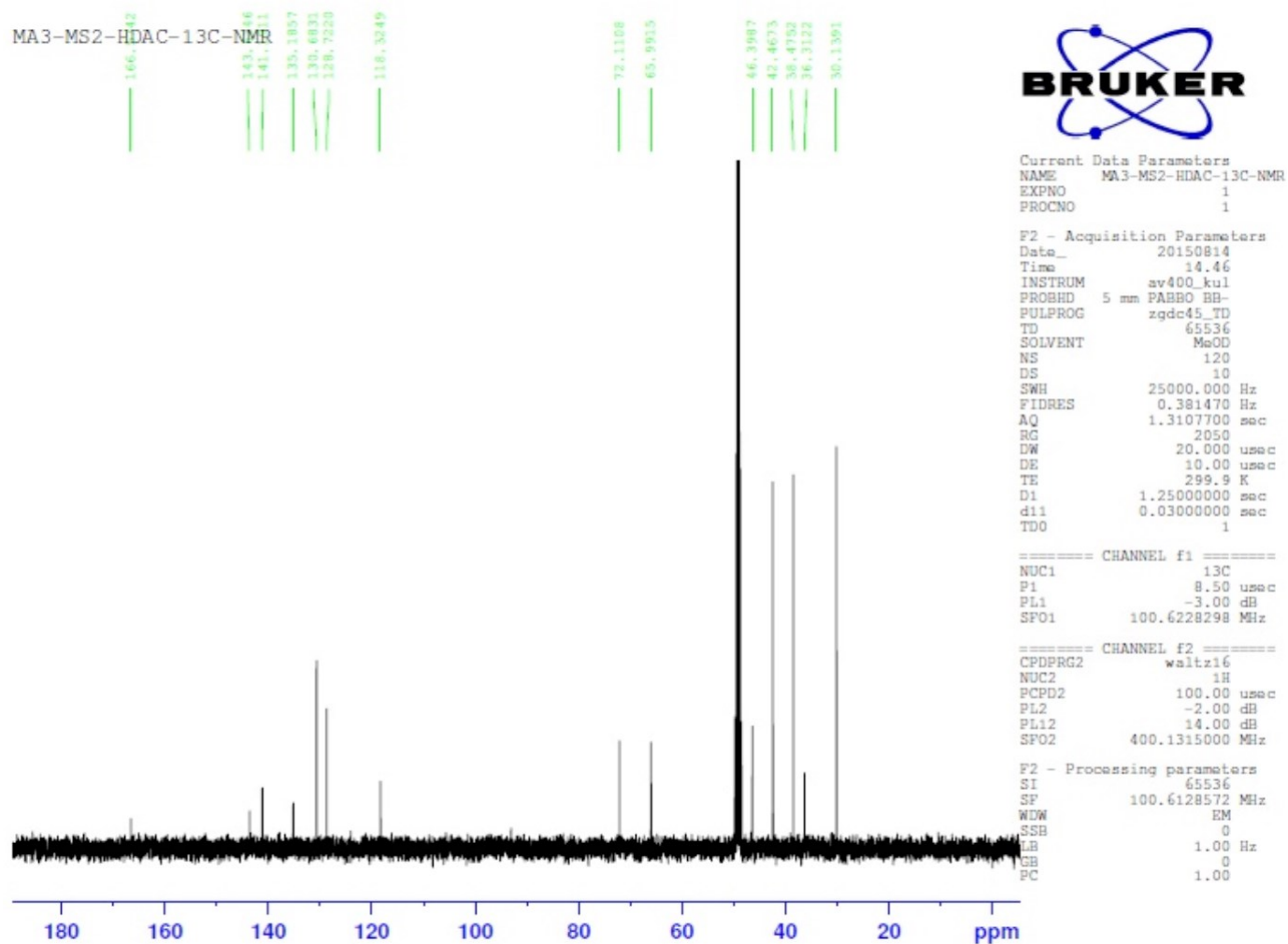
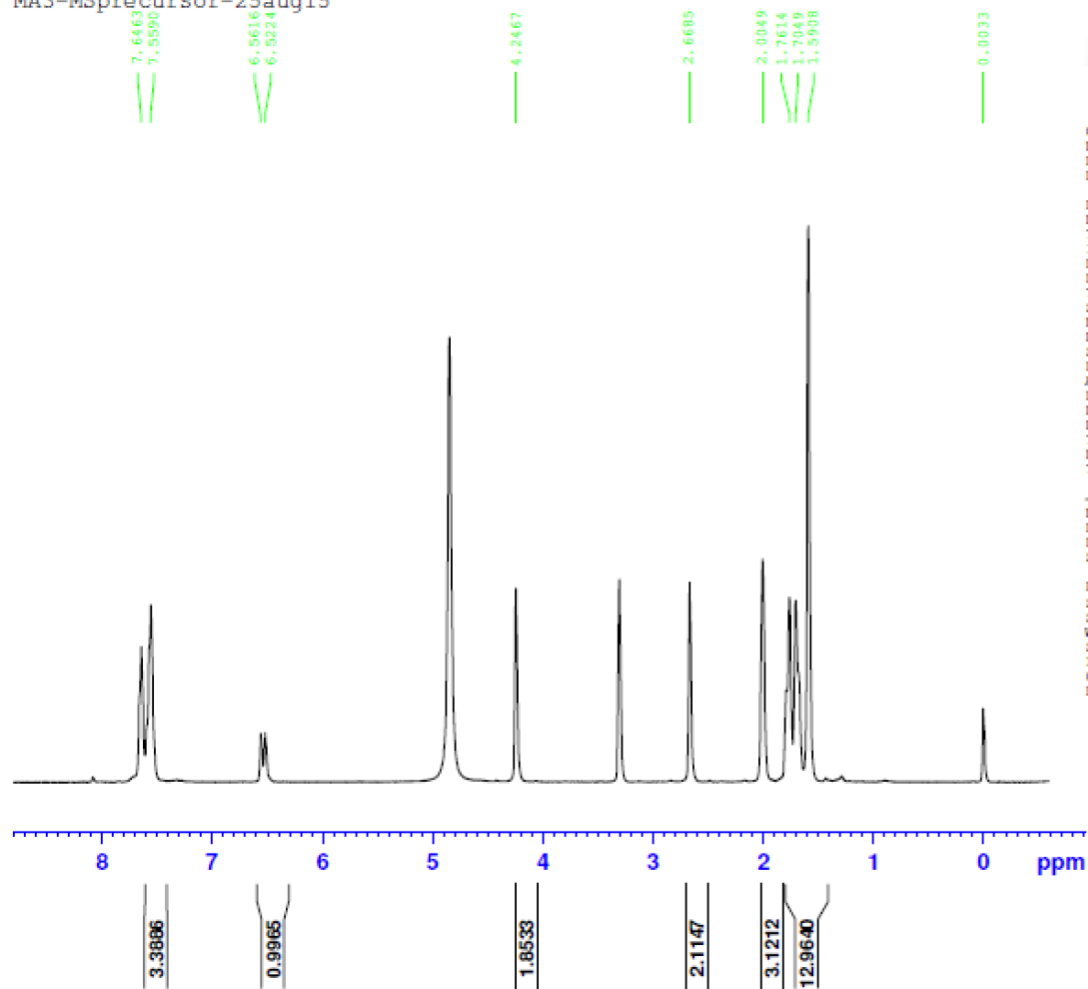


Figure S3: ^{13}C -NMR spectrum of martinostat (**3**) in CD_3OD .

MA3-MSprecursor-25aug15



Current Data Parameters
NAME MA3-MSprecursor-25aug15
EXPNO 2
PROCNO 1

F2 - Acquisition Parameters
Date_ 20150825
Time 10.59
INSTRUM av400_kul
PROBHD 5 mm PABBO HB-
PULPROG zg
TD 32768
SOLVENT MeOD
NS 16
DS 1
SWE 4795.396 Hz
FIDRES 0.146344 Hz
AQ 3.4166601 sec
RG 16
DW 104.267 usec
DE 10.00 usec
TE 300.0 K
D1 5.00000000 sec
TDO 1

----- CHANNEL f1 -----
NUC1 1H
P1 6.50 usec
PL1 -2.00 dB
SFO1 400.1337395 MHz

F2 - Processing parameters
SI 32768
SF 400.1315802 MHz
WDW EM
SSB 0
LB 0.30 Hz
GB 0
PC 1.40

Figure S4: ¹H-NMR spectrum of *N*-desmethyl-martinostat (**2**) in CDCl₃.

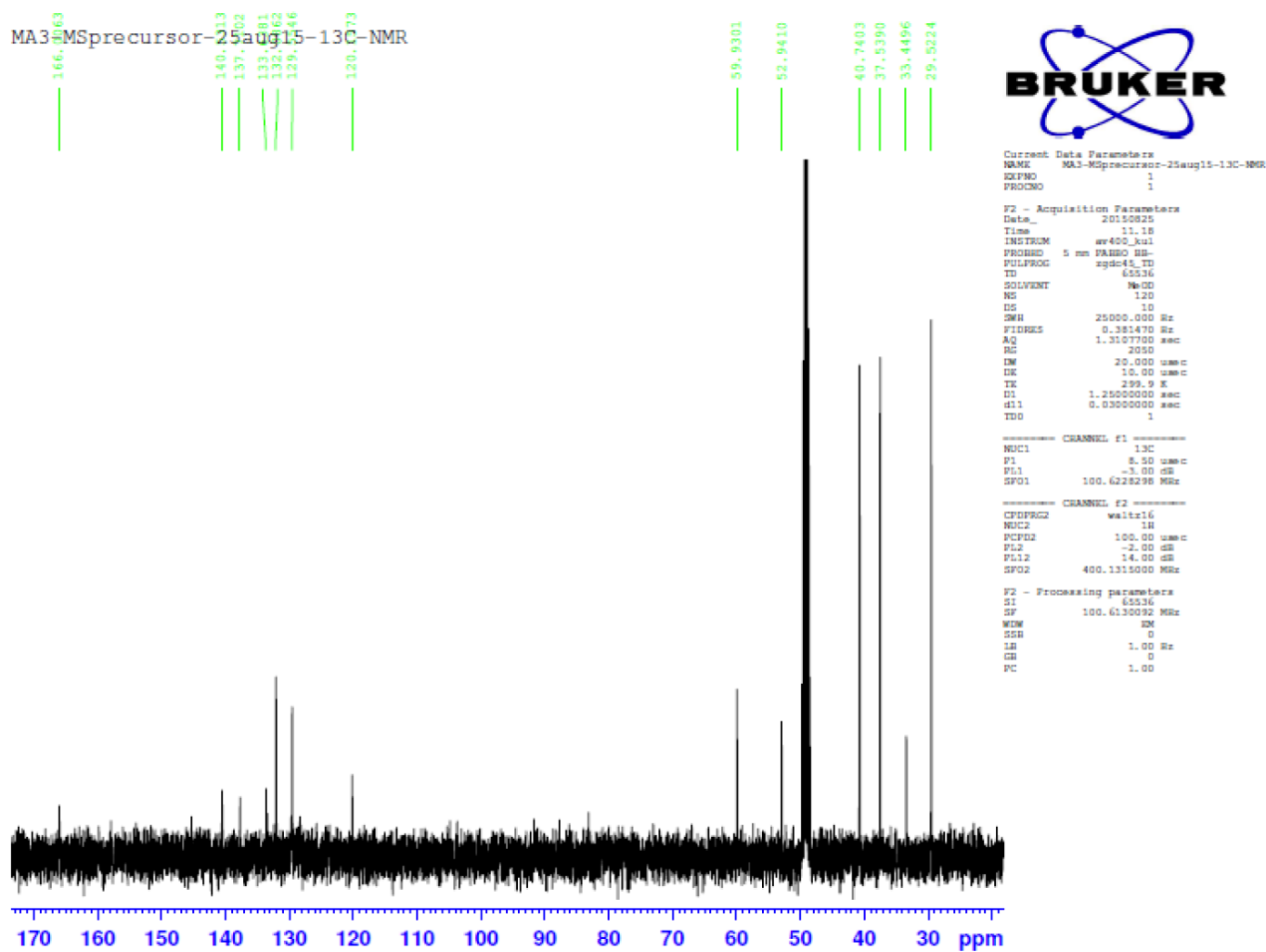


Figure S5: ^{13}C -NMR spectrum of *N*-desmethyl-martinostat (**2**) in CDCl_3 .

MA3-HDAC-MS-FEt-NHOH

7.4713
7.2944
7.2519
7.2351
6.4164
6.3752
6.3355

4.5645
4.5300
4.5344
4.2628
4.2006
4.1430

1.7973
1.7690
1.6716
1.5649
1.1891



Current Data Parameters
NAME MA3-HDAC-MS-FEt-NHOH
EXPNO 1
PROCNO 1

F2 - Acquisition Parameters
Date_ 20150602
Time 10.46
INSTRUM av400_kul
PROBHD 5 mm PABBO BB-
PULPROG zg
TD 32768
SOLVENT MeOD
NS 16
DS 4
SWH 6009.615 Hz
FIDRES 0.183399 Hz
AQ 2.7263477 sec
RG 203
DW 83.200 usec
DE 10.00 usec
TE 296.5 K
D1 5.0000000 sec
TDO 1

==== CHANNEL f1 =====
NUC1 1H
P1 6.50 usec
PL1 -2.00 dB
SFO1 400.1328553 MHz

F2 - Processing parameters
SI 32768
SF 400.1310007 MHz
WDW EM
SSB 0
LB 0.30 Hz
GB 0
PC 1.40

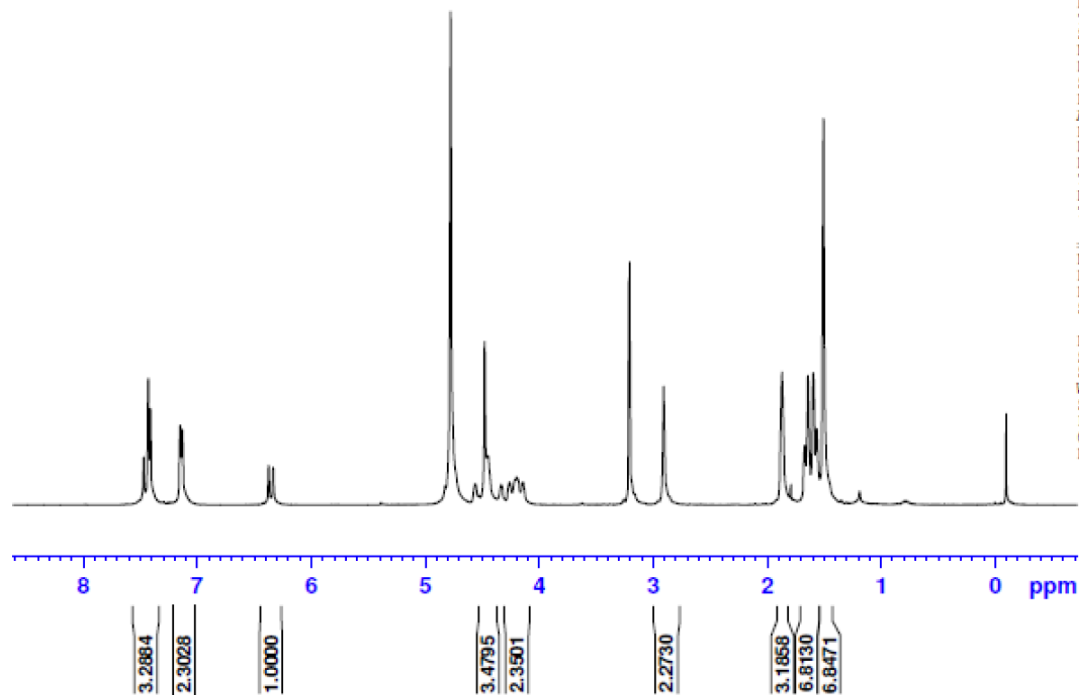


Figure S6: ¹H-NMR spectrum of fluoroethyl-martinostat (**4**) in CD₃OD.

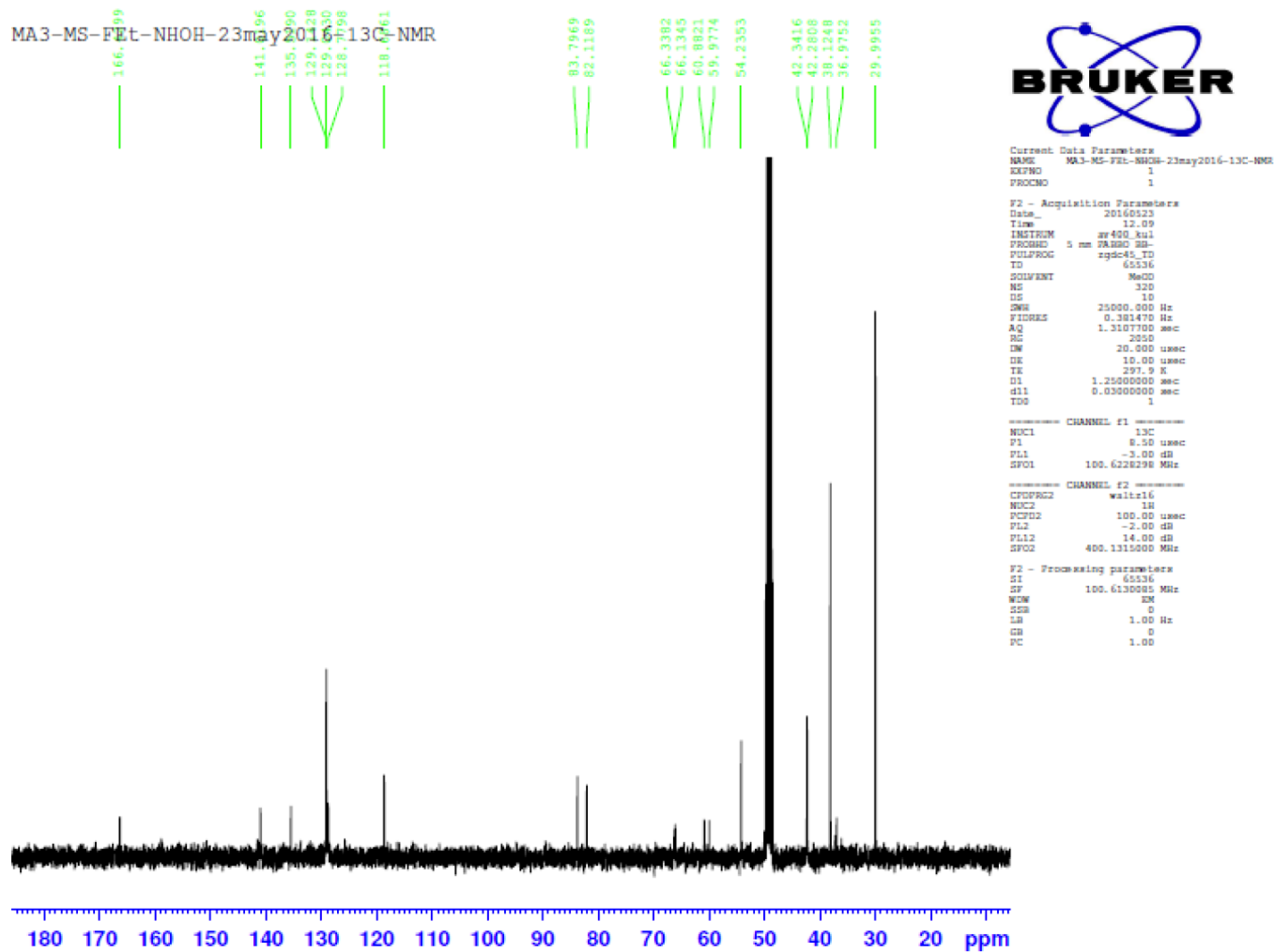


Figure S7: ¹³C-NMR spectrum of fluoroethyl-martinostat (**4**) in CD₃OD.

MA3-HDAC-S3-final

7.6064
7.6060
7.5810
7.5794
7.5094
7.5070
7.4961
7.4708
7.4728
7.4235
7.4207
7.3976
7.3957
7.3738
7.3716
7.3562
7.3400
7.3243
7.3220
7.0941
7.0908
7.0685
7.0675
7.0451
7.0419
7.0059
6.9985
6.9933
6.9816
6.9764
6.9691



Current Data Parameters
NAME MA3-HDAC-S3-final
EXPNO 2
PROCNO 1

F2 - Acquisition Parameters
Date_ 20140827
Time 11.03
INSTRUM av400_kul
PROBHD 5 mm PABBO BB-
PULPROG zg
TD 32768
SOLVENT CDCl3
NS 16
DS 4
SWH 6009.615 Hz
FIDRES 0.183399 Hz
AQ 2.7263477 sec
RG 64
DW 83.200 usec
DE 10.00 usec
TE 298.0 K
D1 5.0000000 sec
TD0 1

==== CHANNEL f1 =====
NUC1 1H
P1 6.50 usec
PL1 -2.00 dB
SFO1 400.1305687 MHz

F2 - Processing parameters
SI 32768
SF 400.1284294 MHz
WDW EM
SSB 0
LB 0.30 Hz
GB 0
PC 1.40

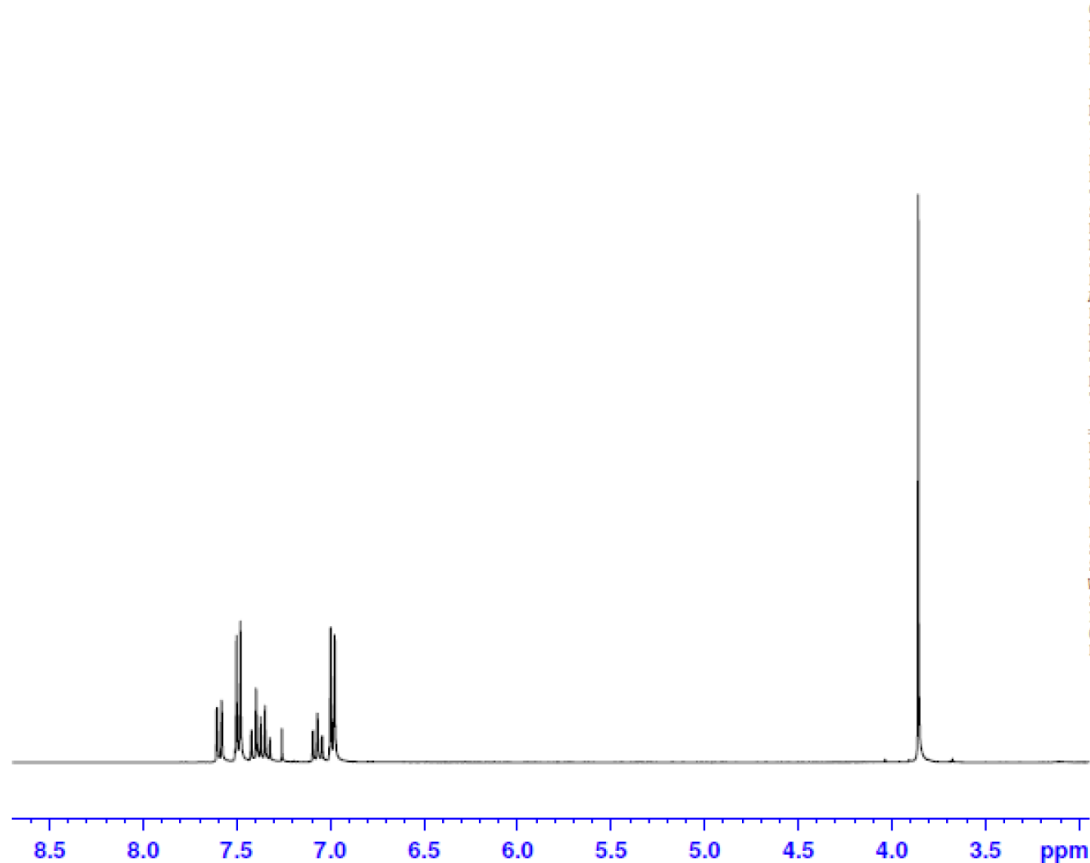


Figure S8: ¹H-NMR spectrum of α -(4-methoxyphenyl) tropolone (**7**) in CDCl₃.

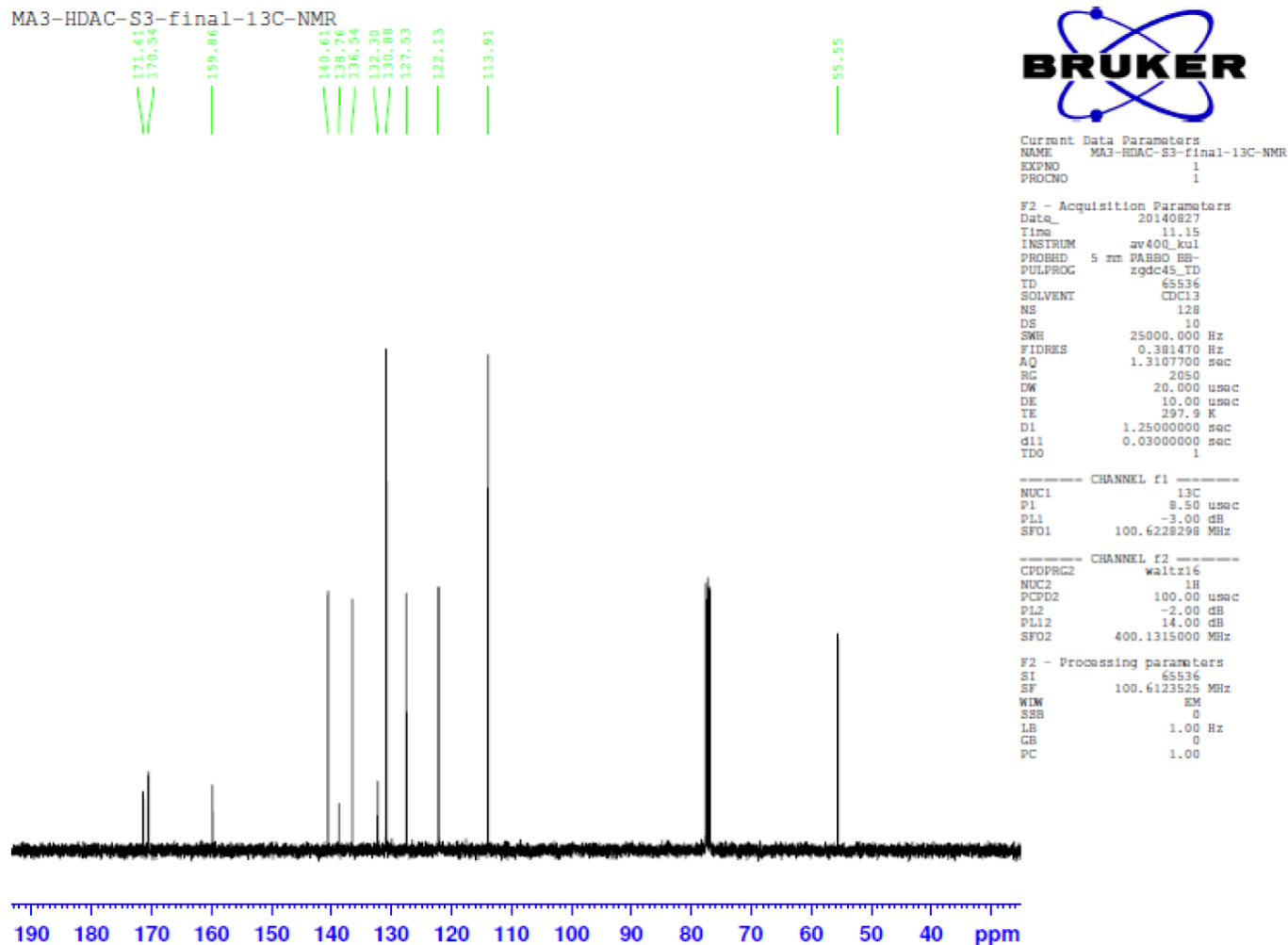
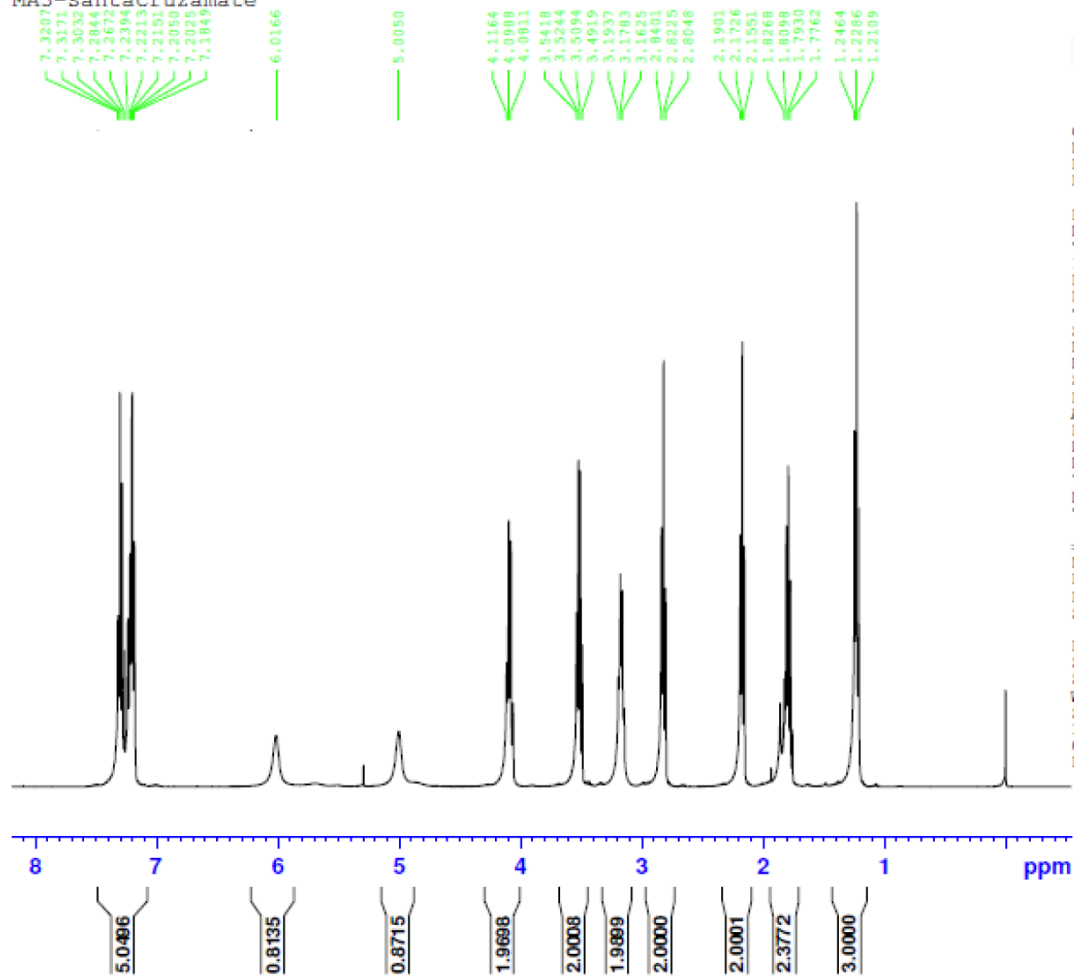


Figure S9: ^{13}C -NMR spectrum of α -(4-methoxyphenyl) tropolone (**7**) in CDCl_3 .

MA3-santacruzamate



Current Data Parameters
NAME MA3-santacruzamate
EXPNO 1
PROCNO 1

F2 - Acquisition Parameters
Date_ 20150814
Time 11.00
INSTRUM av400_kul
PROBHD 5 mm PABBO BB-
PULPROG zg
TD 32768
SOLVENT CDC13
NS 16
DS 4
SWH 6009.615 Hz
FIDRES 0.183399 Hz
AQ 2.7263477 sec
RG 64
DW 83.200 usec
DE 10.00 usec
TE 300.0 K
D1 5.0000000 sec
TD0 1

==== CHANNEL f1 =====
NUC1 1H
P1 6.50 usec
PL1 -2.00 dB
SFO1 400.1305687 MHz

F2 - Processing parameters
SI 32768
SF 400.1300020 MHz
WDW EM
SSB 0
LB 0.30 Hz
GB 0
PC 1.40

Figure S10: ¹H-NMR spectrum of santacruzamate A (5) in CDCl₃.

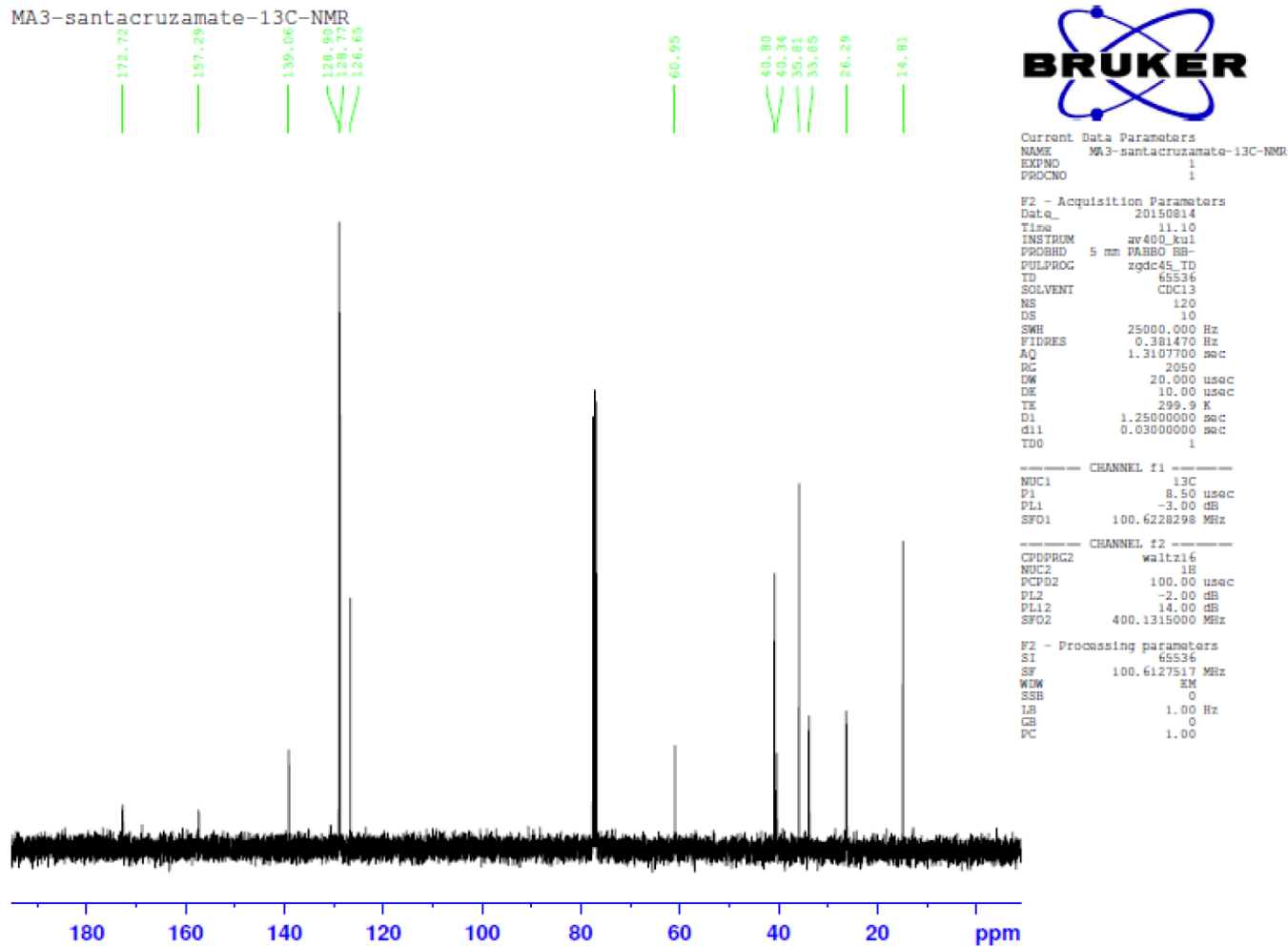
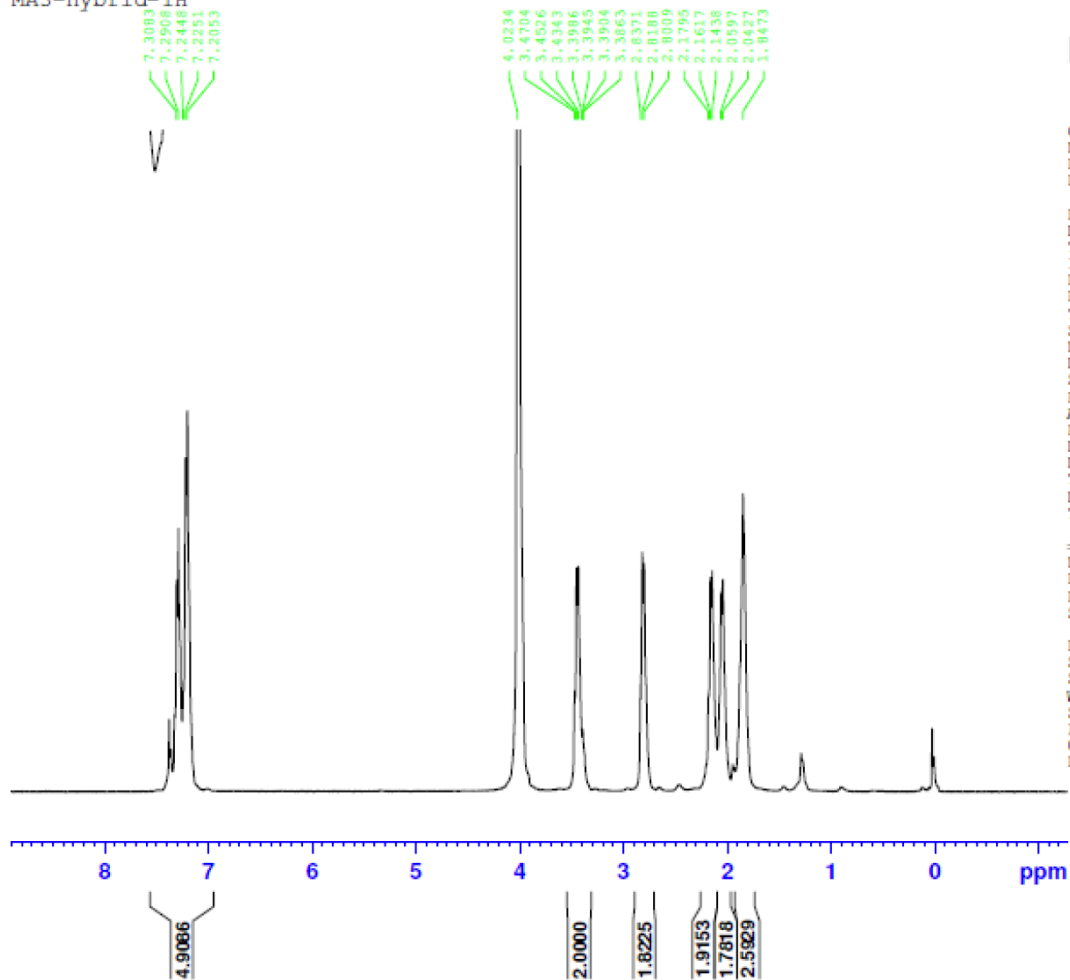


Figure S11: ¹³C-NMR spectrum of santacruzamate A (5) in CDCl₃.

MA3-hybrid-1H



Current Data Parameters
NAME MA3-hybrid-1H
EXPNO 1
PROCNO 1

F2 - Acquisition Parameters
Date_ 20150814
Time 11.26
INSTRUM av400_kul
PROBHD 5 mm PABBO BB-
PULPROG zg
TD 32768
SOLVENT CDC13
NS 16
DS 4
SWH 6009.615 Hz
FIDRES 0.183399 Hz
AQ 2.7263477 sec
RG 64
DW 83.200 usec
DE 10.00 usec
TE 300.0 K
D1 5.00000000 sec
TD0 1

==== CHANNEL f1 =====
NUC1 1H
P1 6.50 usec
PL1 -2.00 dB
SFO1 400.1319789 MHz

F2 - Processing parameters
SI 32768
SF 400.1299605 MHz
WDW EM
SSB 0
LB 0.30 Hz
GB 0
PC 1.40

Figure S12: ¹H-NMR spectrum of santacruzamate A-SAHA hybrid (6) in CDCl₃ + CD₃OD.

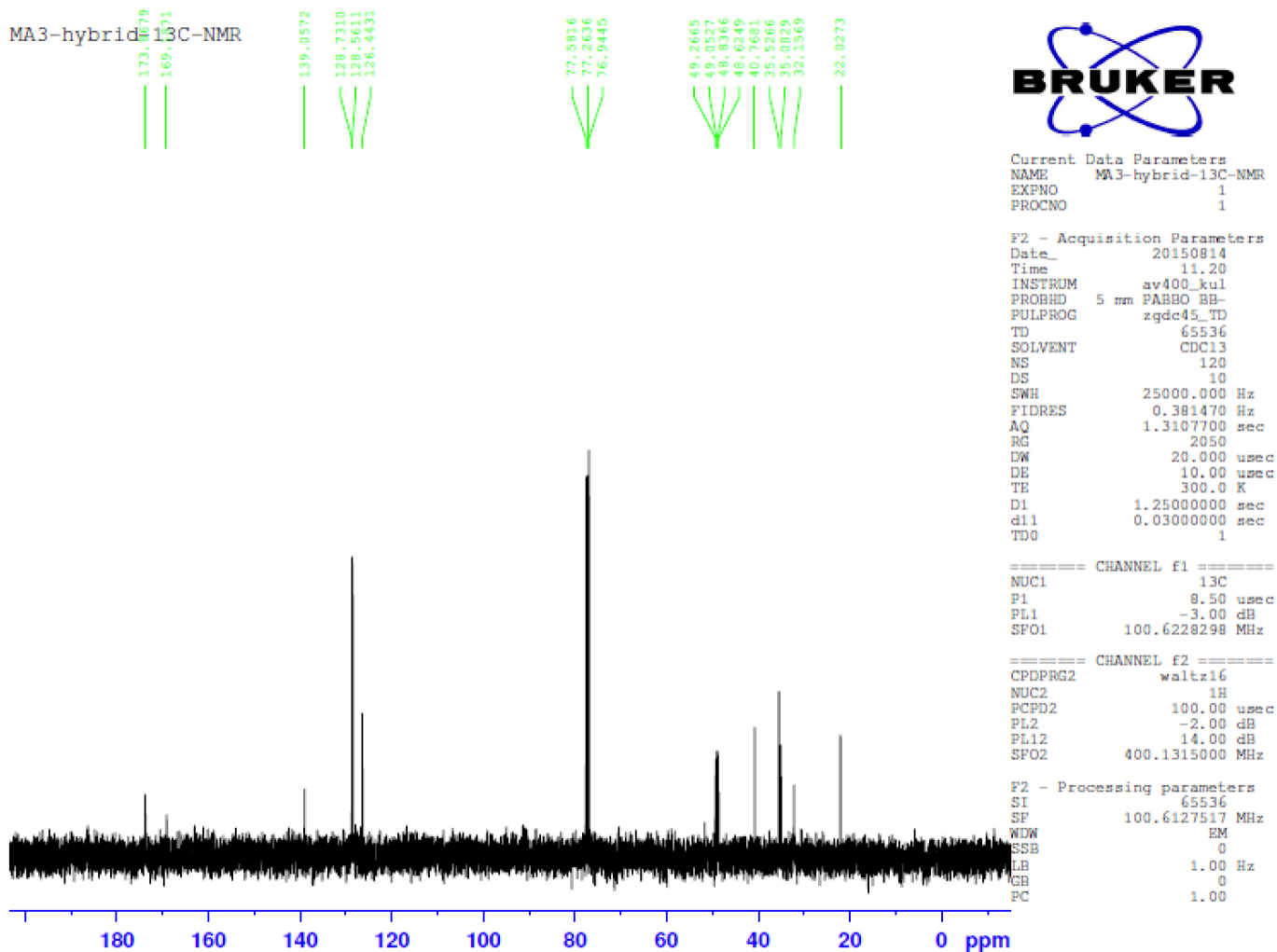


Figure S13: ¹³C-NMR spectrum of santacruzamate A-SAHA hybrid (6) in CDCl₃ + CD₃OD.

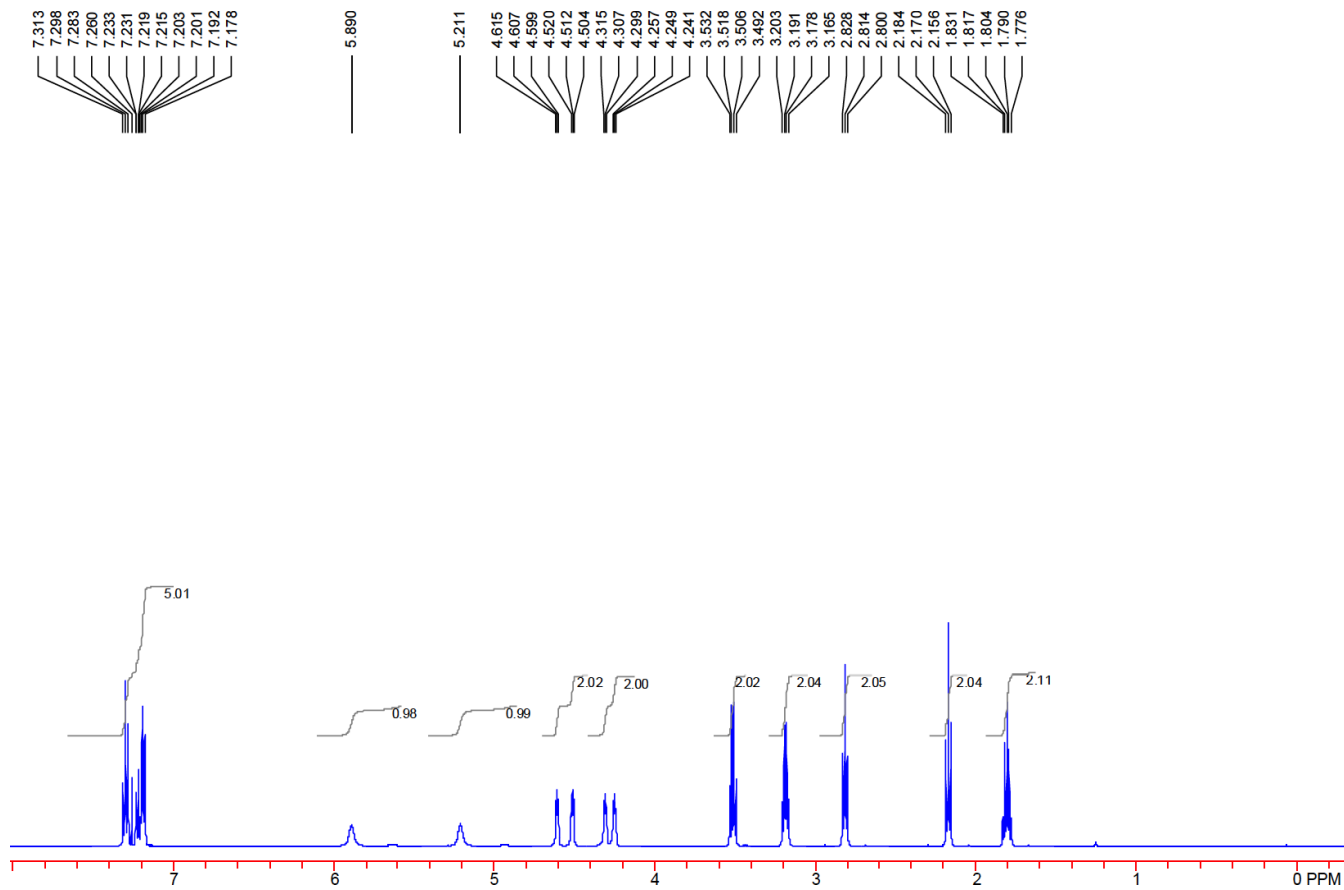


Figure S14: $^1\text{H-NMR}$ spectrum of fluoroethyl-santacruzamate A (**9**) in CDCl_3 .

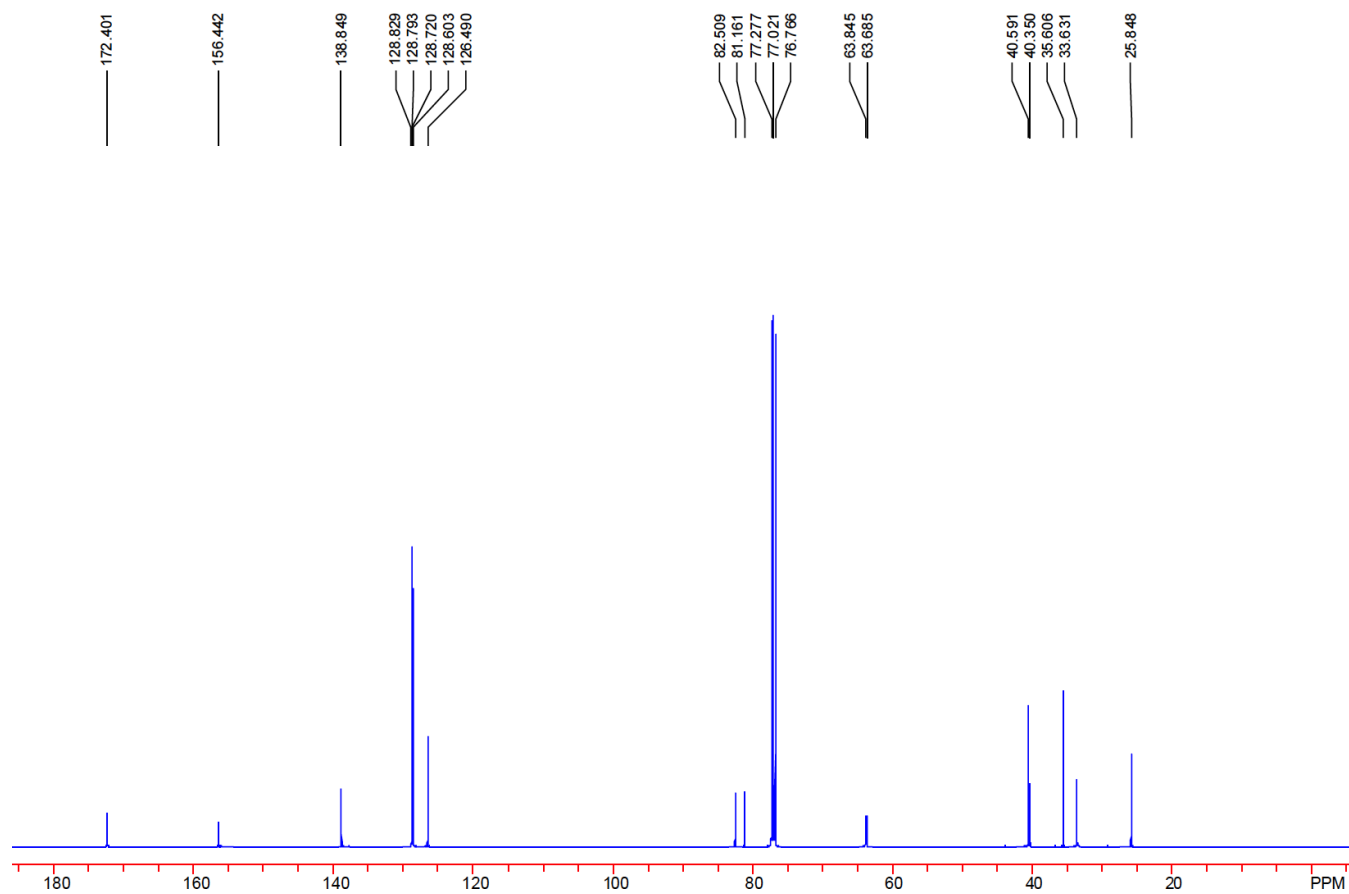


Figure S15: ^{13}C -NMR spectrum of fluoroethyl-santacruzamate (9) in CDCl_3 .

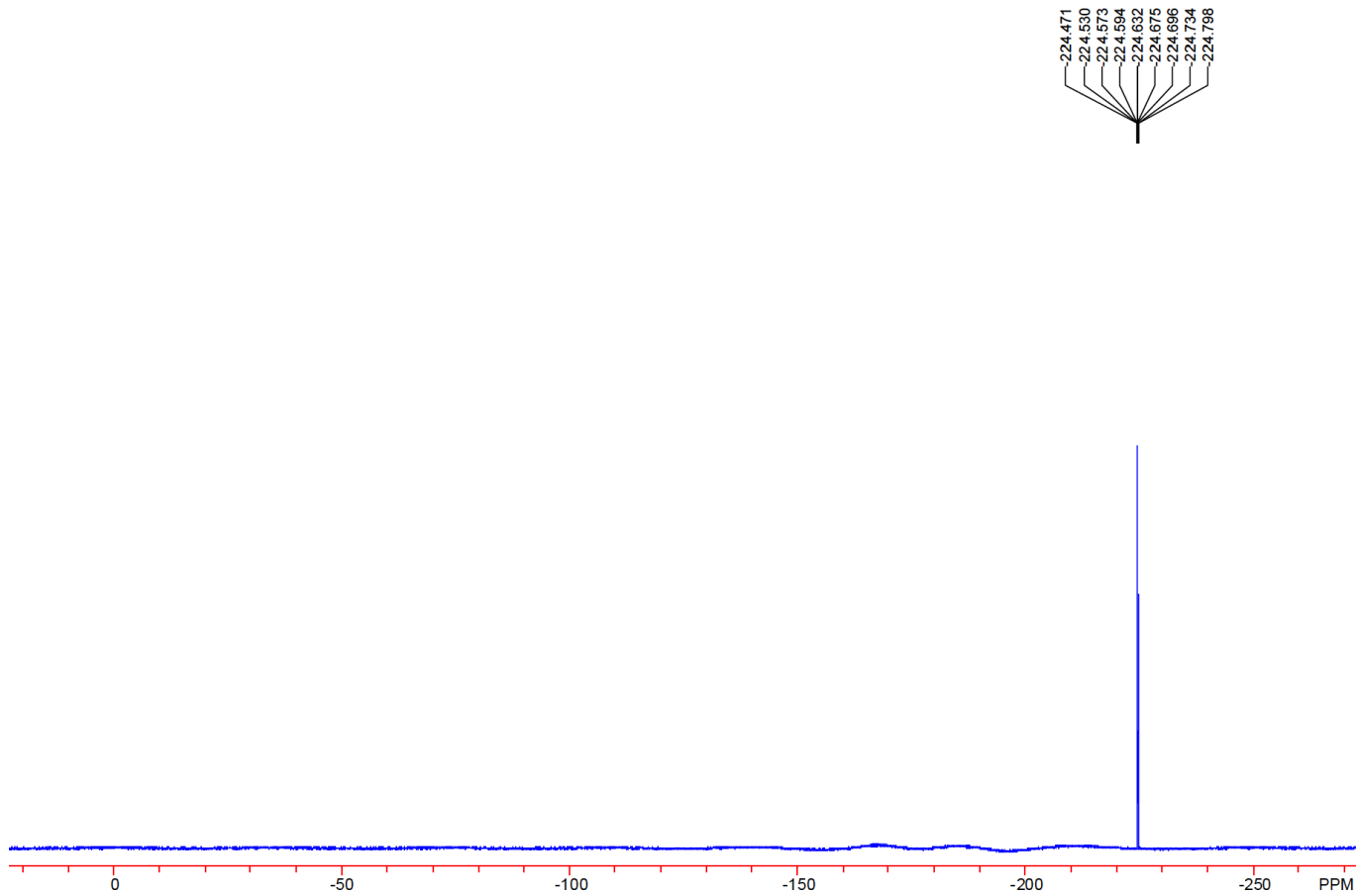


Figure S16: ^{19}F -NMR spectrum of fluoroethyl-santacruzamate (**9**) in CDCl_3 .

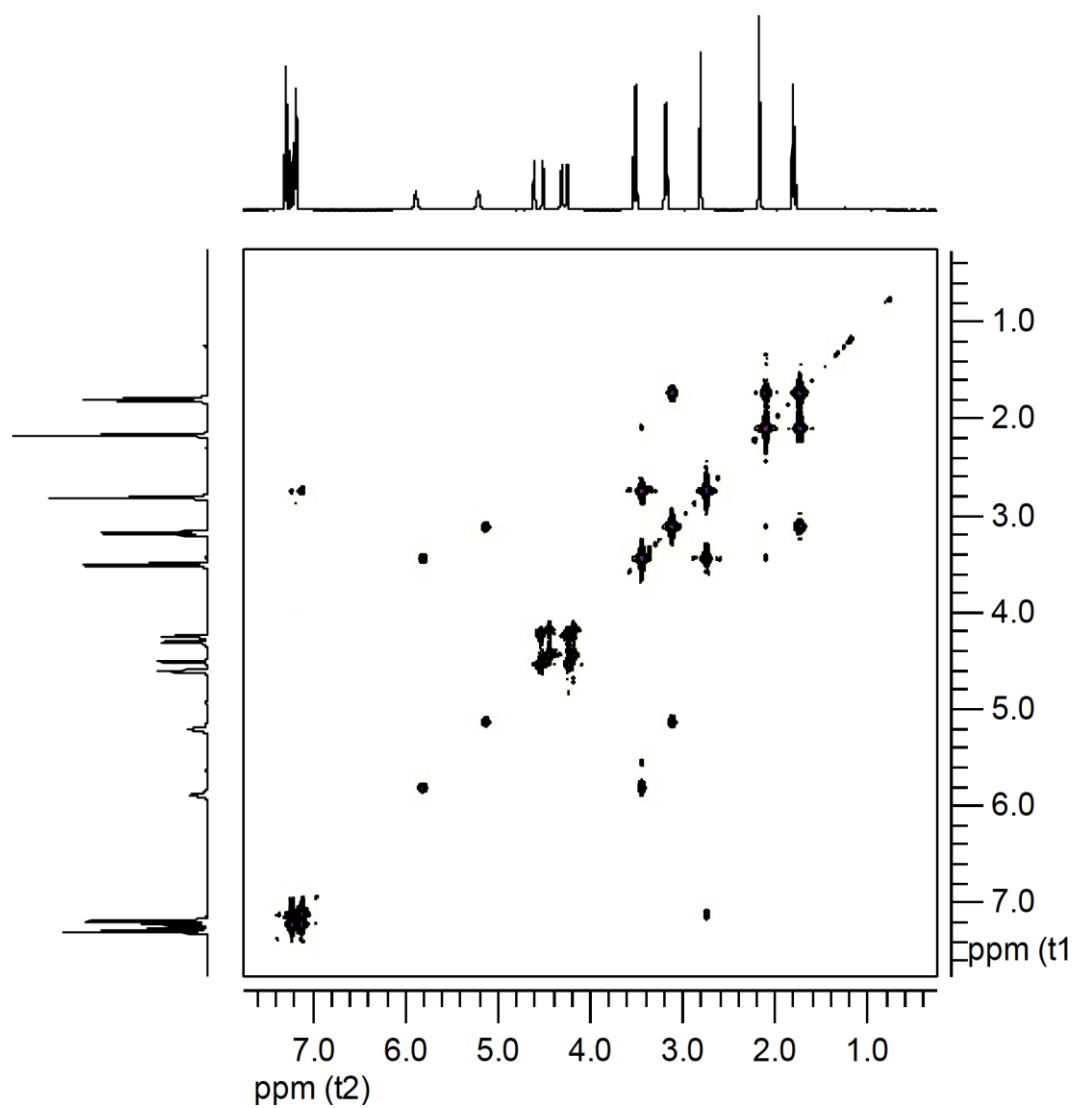


Figure S17: ^1H - ^1H COSY spectrum of fluoroethyl-santacruzamate (9) in CDCl_3 .

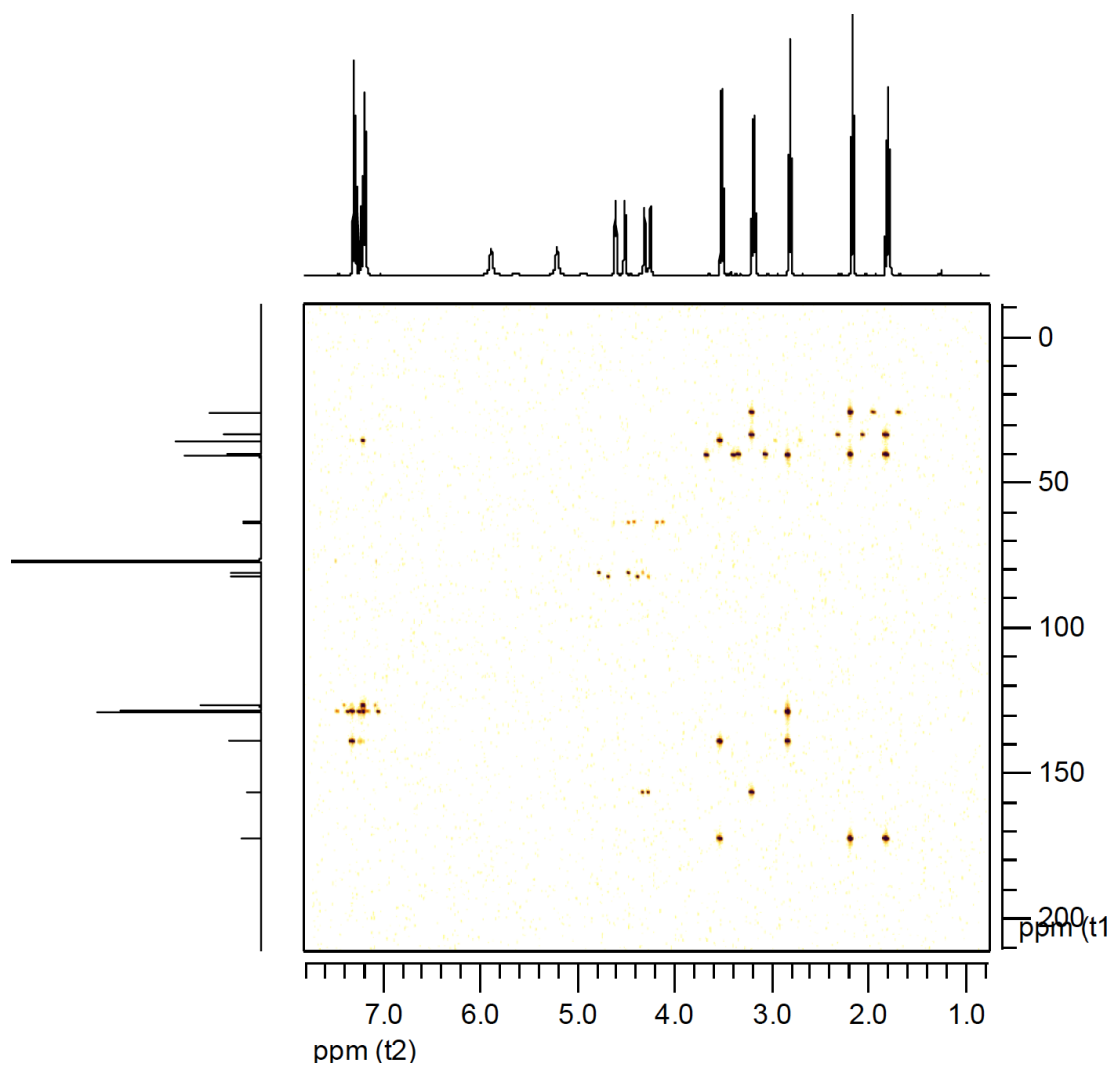


Figure S18: ^1H - ^{13}C HMBC spectrum of fluoroethyl-santacruzamate (**9**) in CDCl_3 .

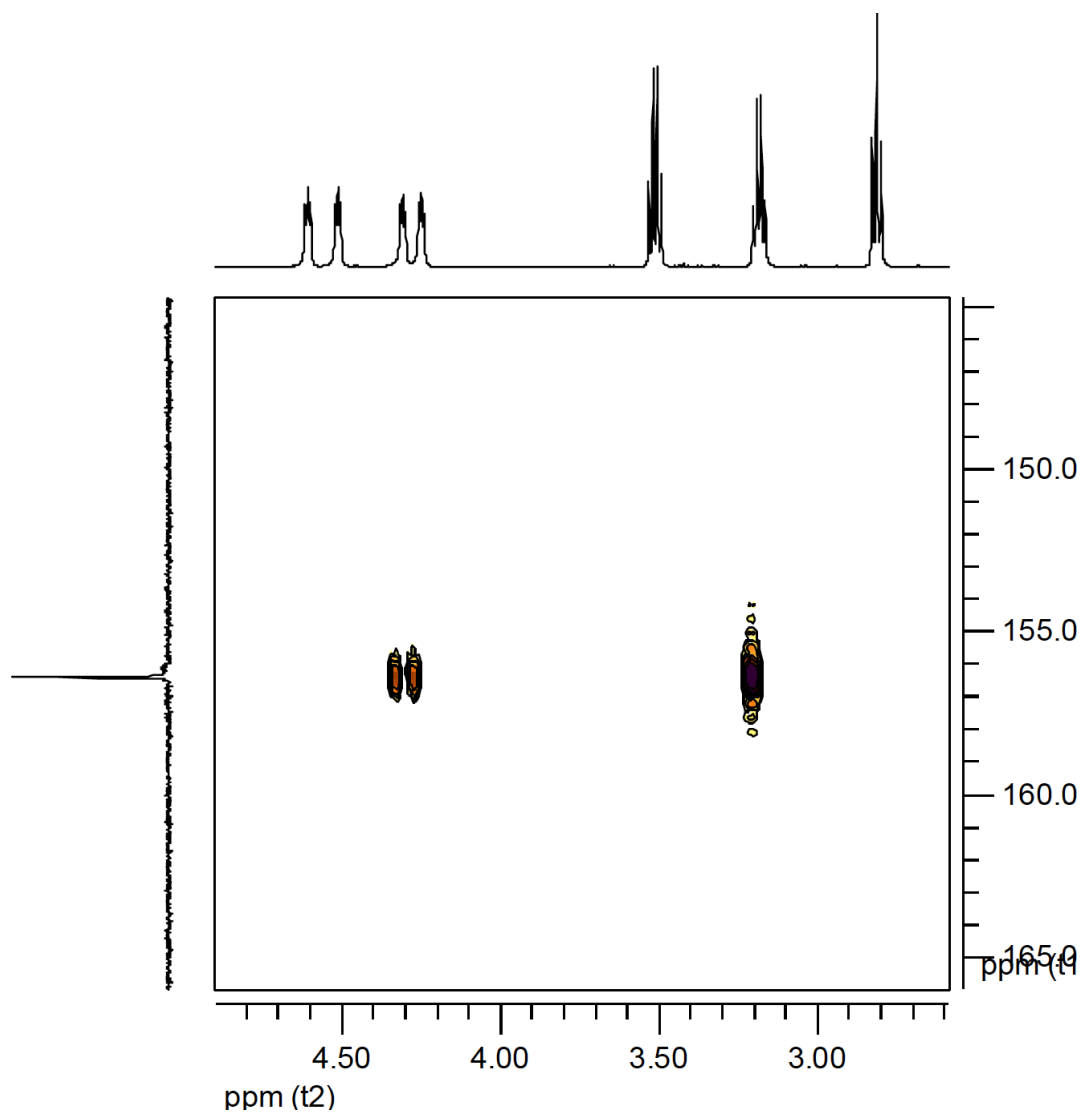


Figure S19: Part of the ^1H - ^{13}C HMBC spectrum of fluoroethyl-santacruzamate-A (**9**) showing correlation to determine the position of the 2- fluoroethyl group and the incorporation of the COO group.

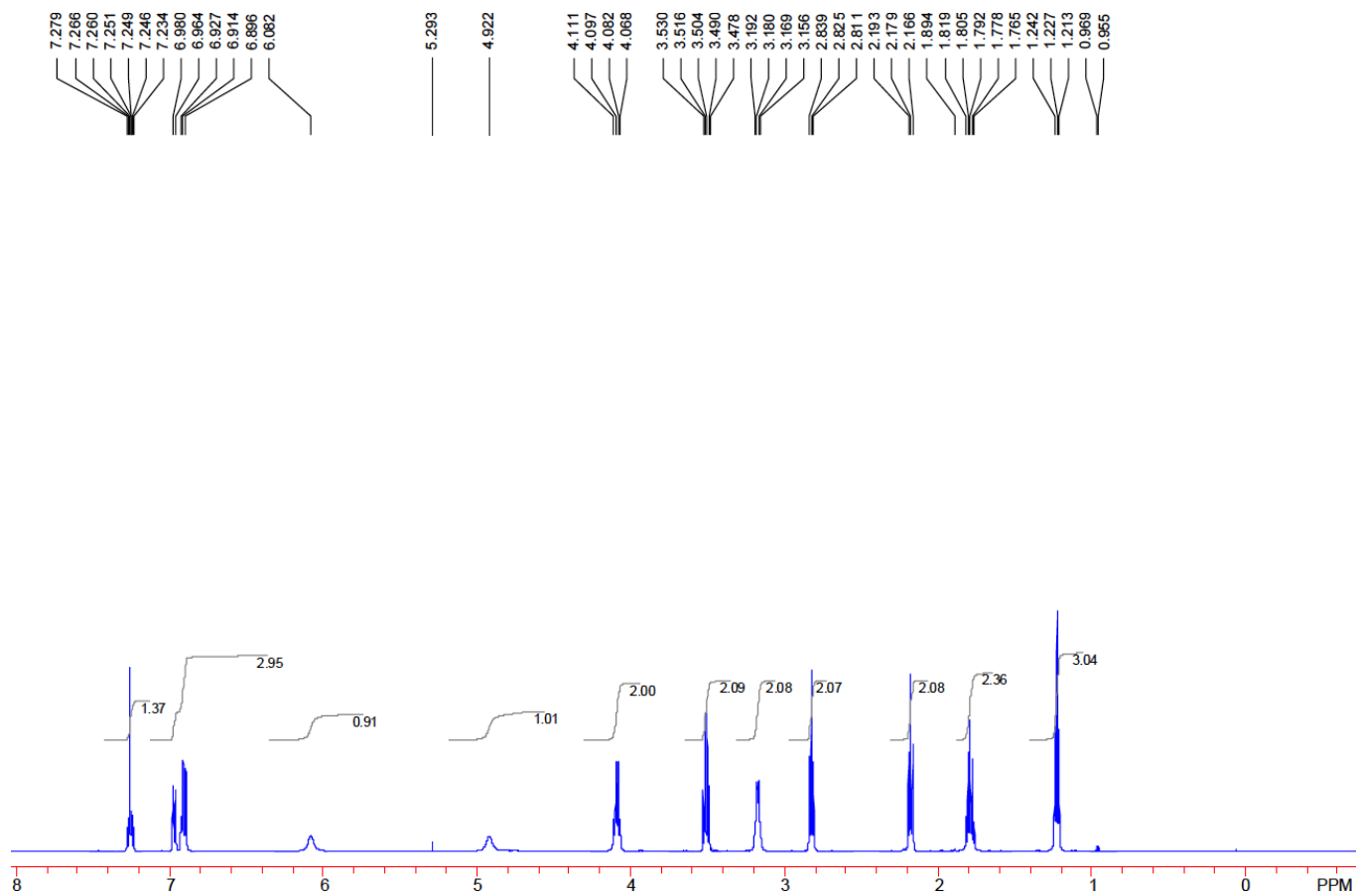


Figure S20: $^1\text{H-NMR}$ spectrum of 3-fluorophenethyl-santacruzamate A (**10**) in CDCl_3 .

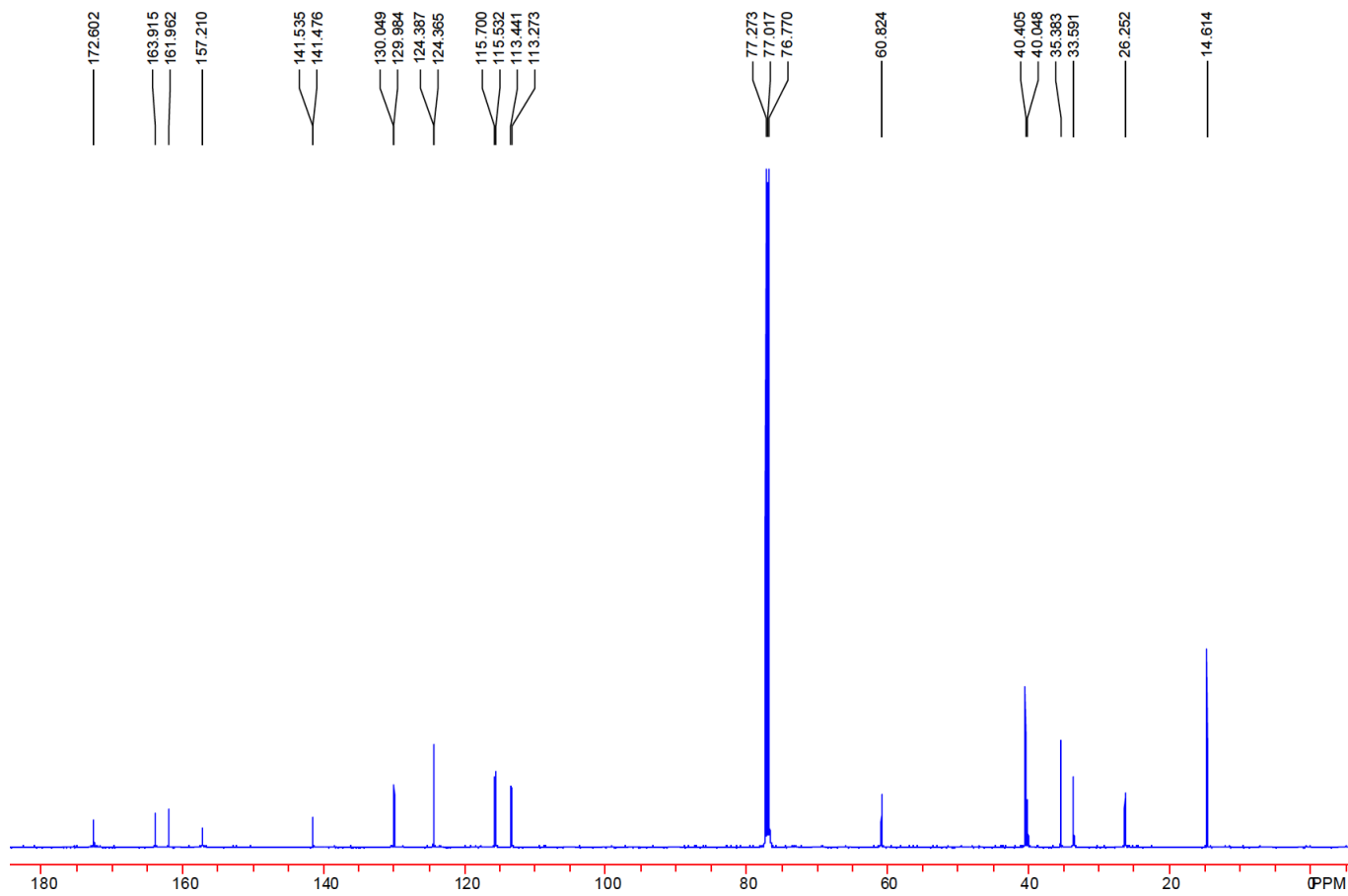


Figure S21: ^{13}C -NMR spectrum of 3-fluorophenethyl-santacruzamate A (**10**) in CDCl_3 .

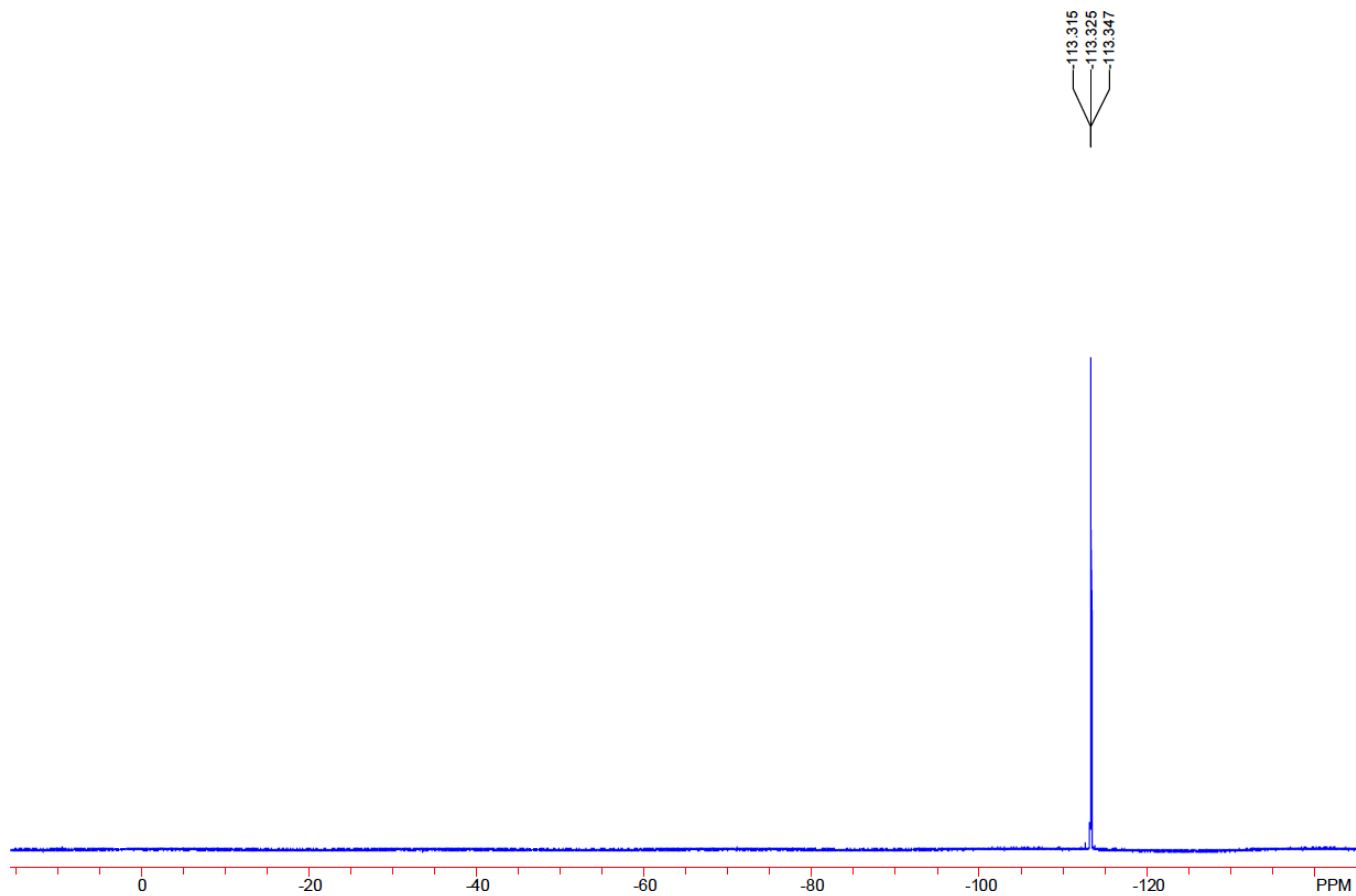


Figure S22: ^{19}F -NMR spectrum of 3-fluorophenethyl-santacruzamate A (**10**) in CDCl_3 .

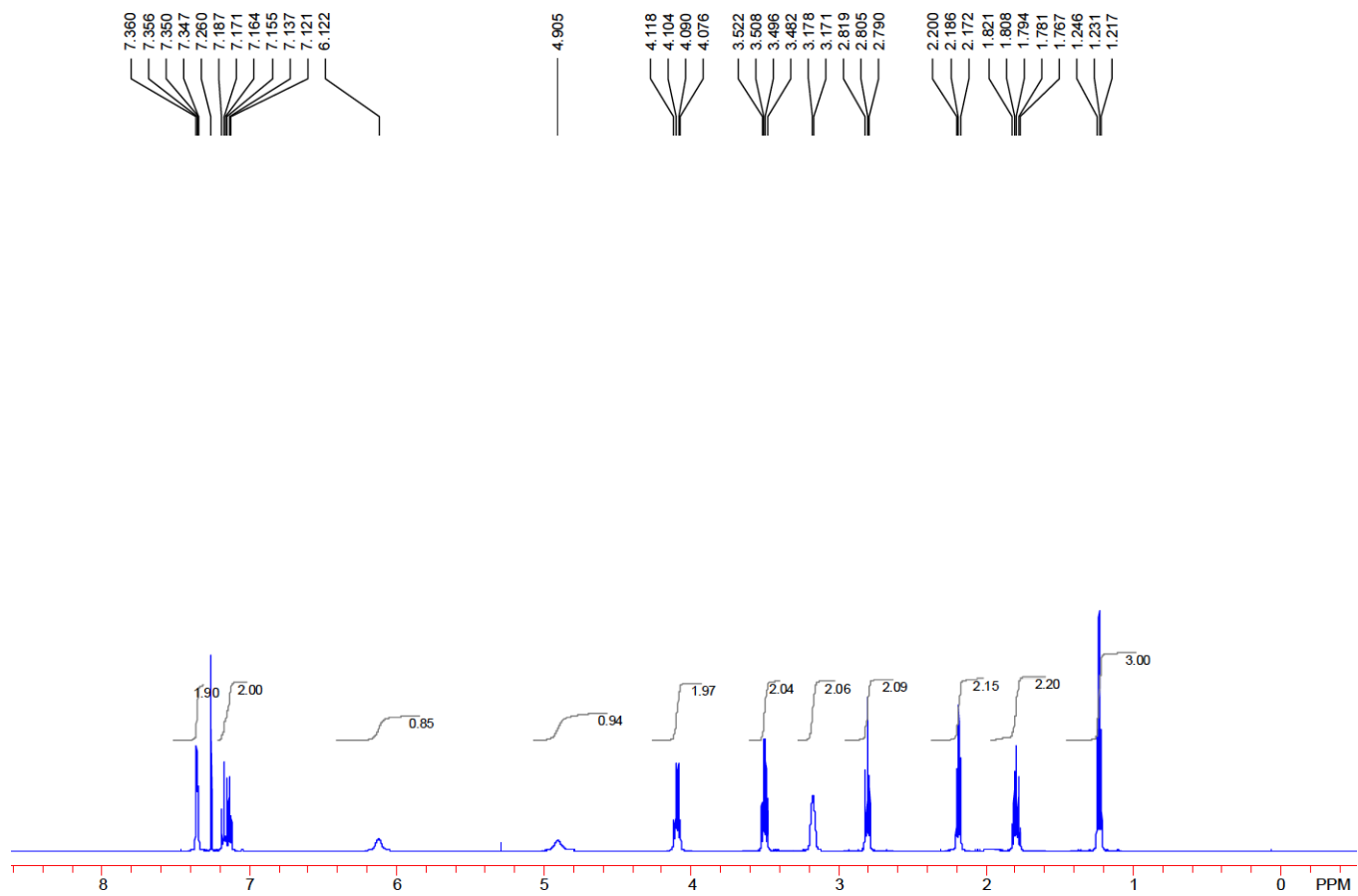


Figure S23: ¹H-NMR spectrum of 3-bromophenethyl-santacruzamate A (**14**) in CDCl₃.

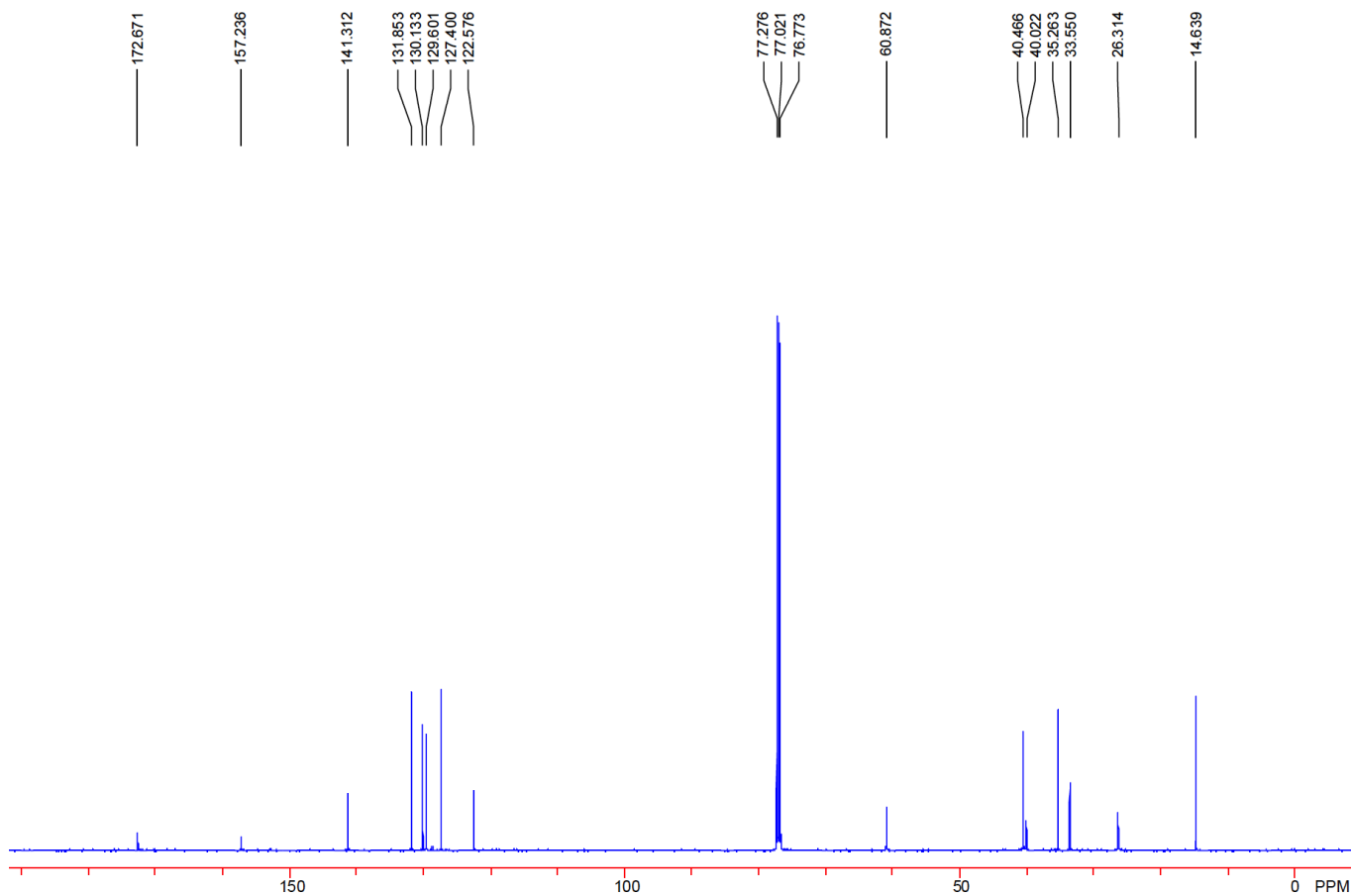


Figure S24: ^{13}C -NMR spectrum of 3-bromophenethyl-santacruzamate A (**14**) in CDCl_3 .

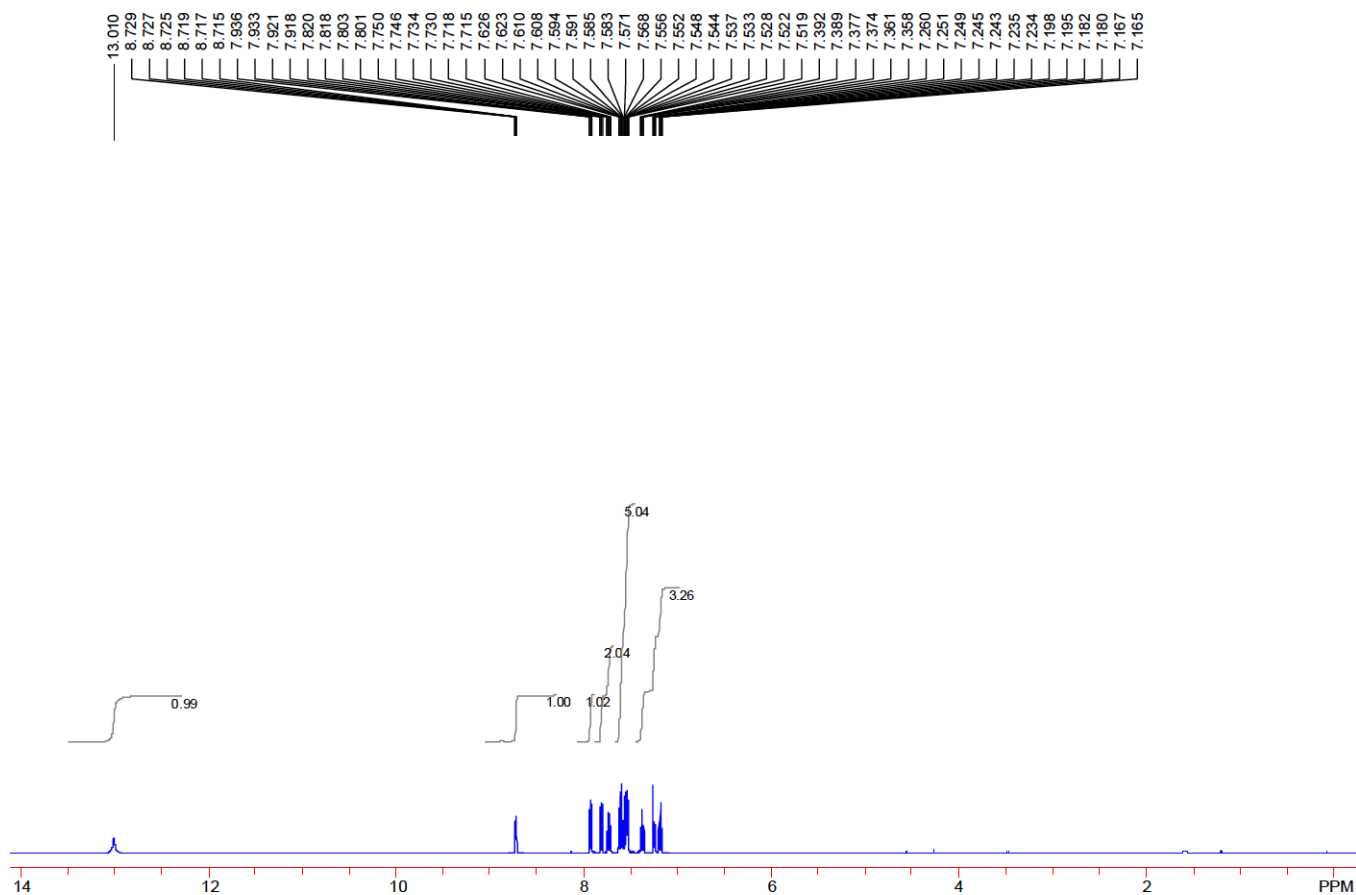


Figure S25: ¹H-NMR spectrum of 2-(2-pyridinyl)-2-nitrobenzenesulfonamide in CDCl₃.

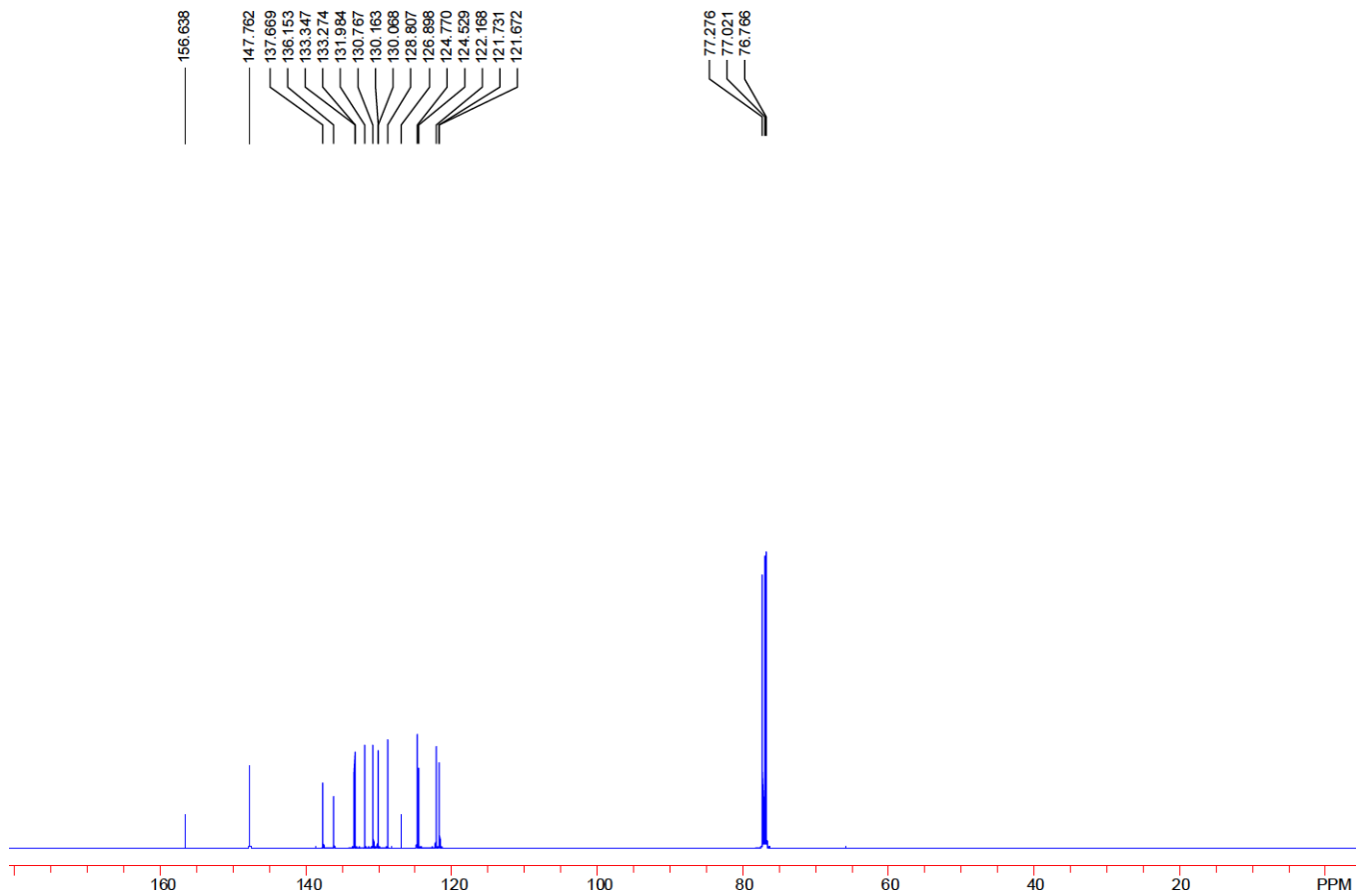


Figure S26: ^{13}C -NMR spectrum of 2-(2-pyridinyl)-2-nitrobenzenesulfonamide in CDCl_3 .

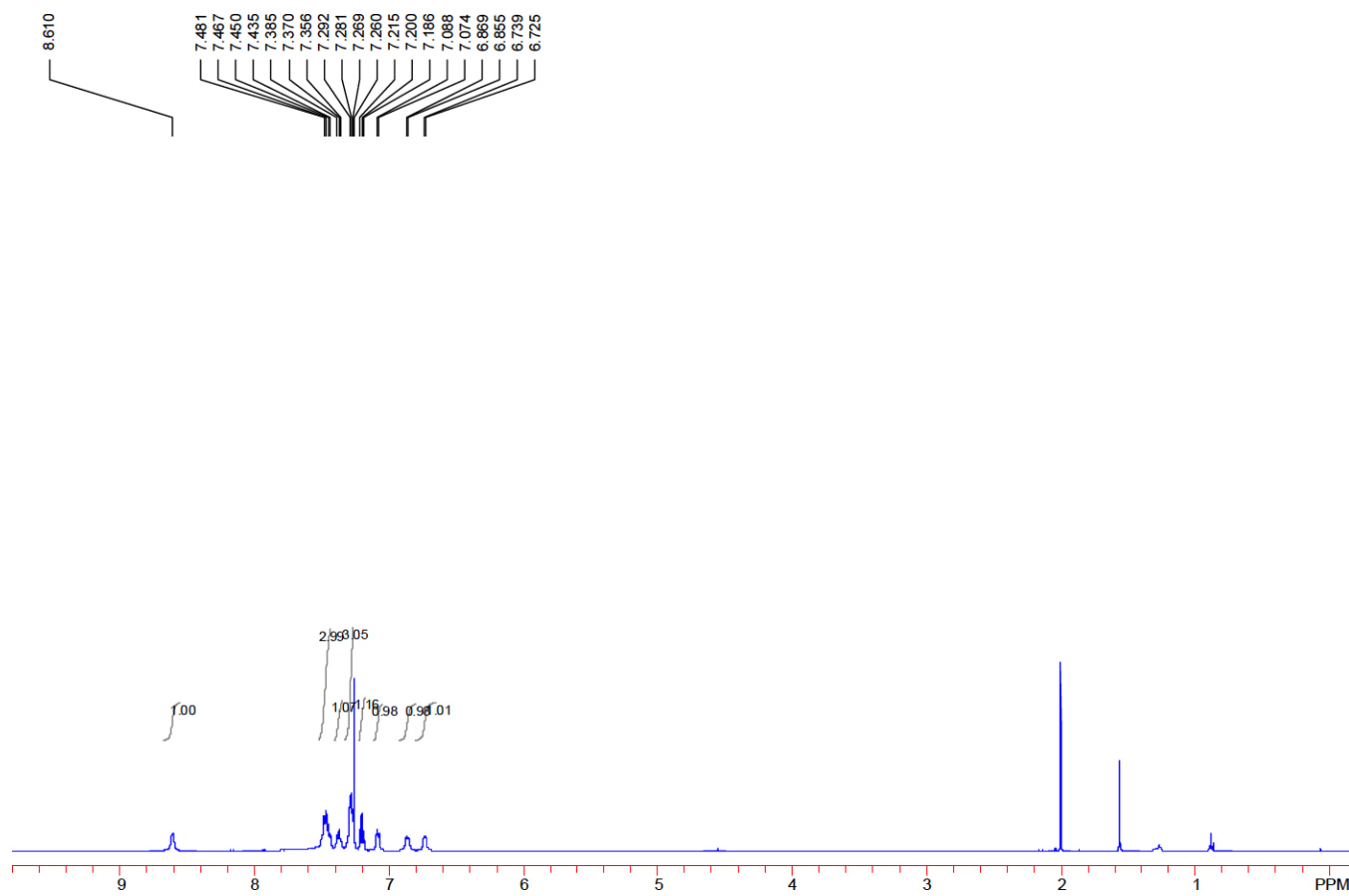


Figure S27: ¹H-NMR spectrum of [2-(2-pyridinyl)-2-nitrobenzenesulfonamide]silver(I) (17) in CDCl₃.

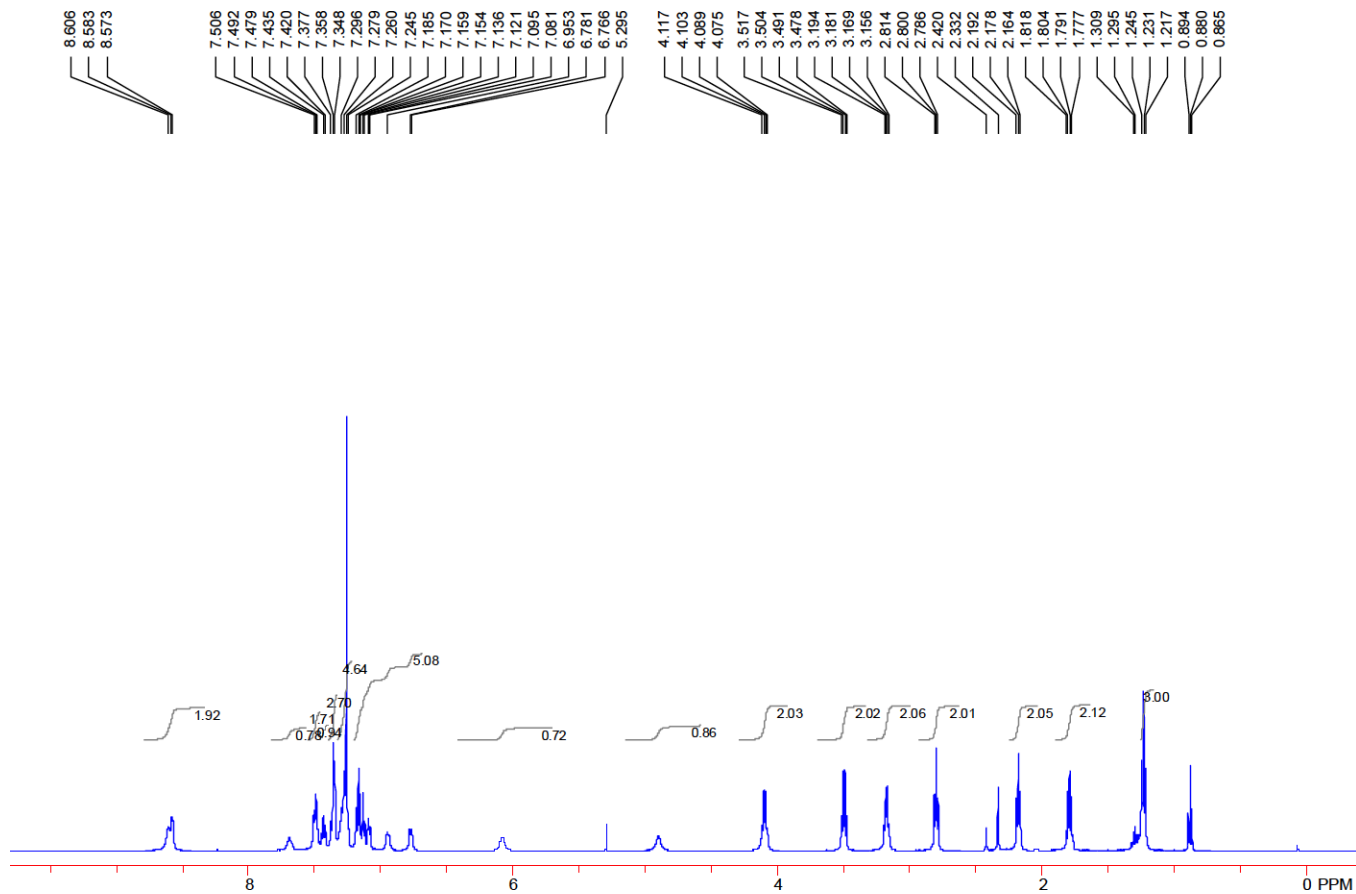


Figure S28: $^1\text{H-NMR}$ spectrum of 3-(phenethyl-Santacruzamate A)-nickel aryl complex (**16**) in CDCl_3 .

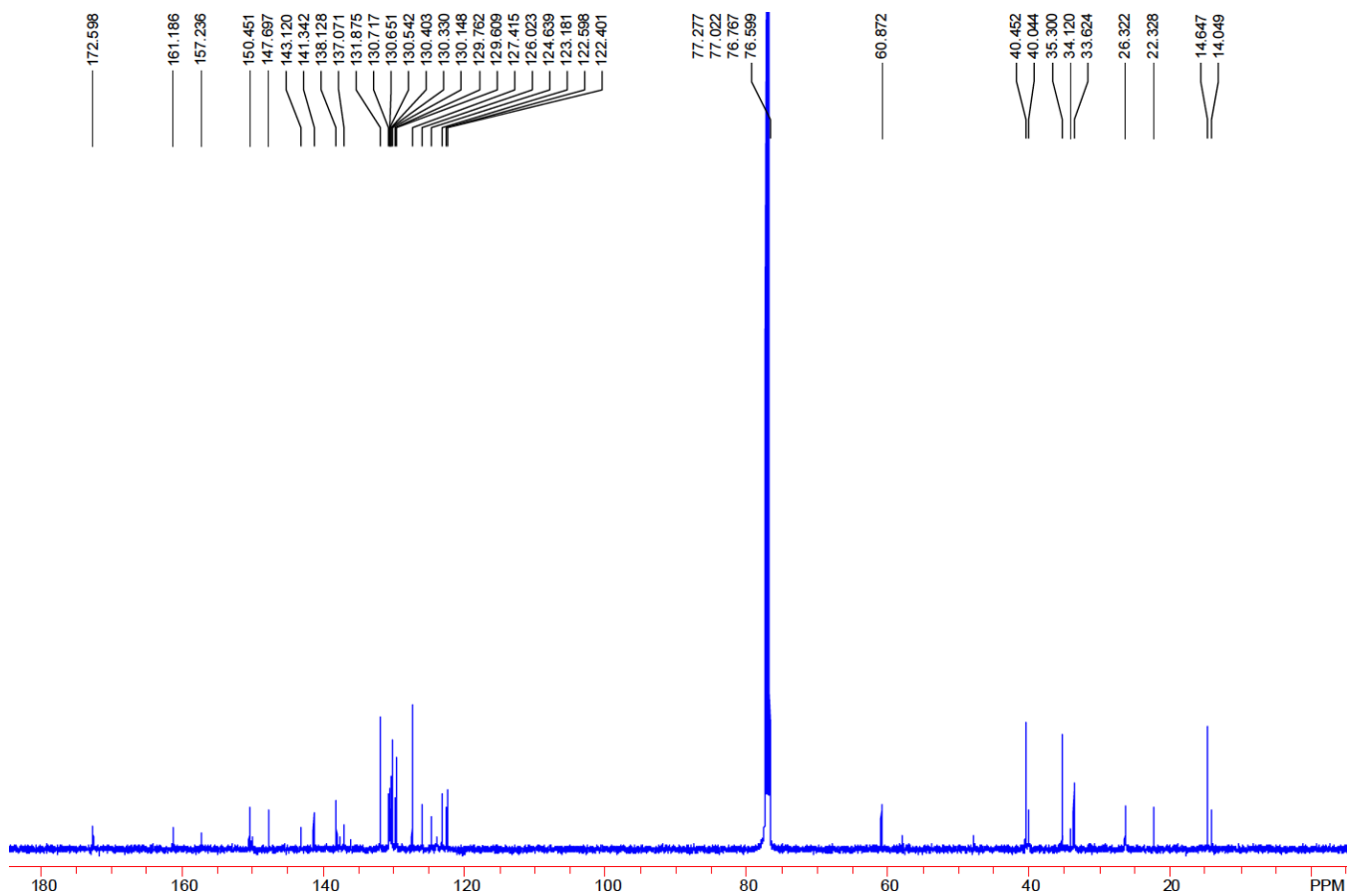


Figure S29: ^{13}C -NMR spectrum of 3-(phenethyl-Santacruzamate A)-nickel aryl complex (**16**) in CDCl_3 .

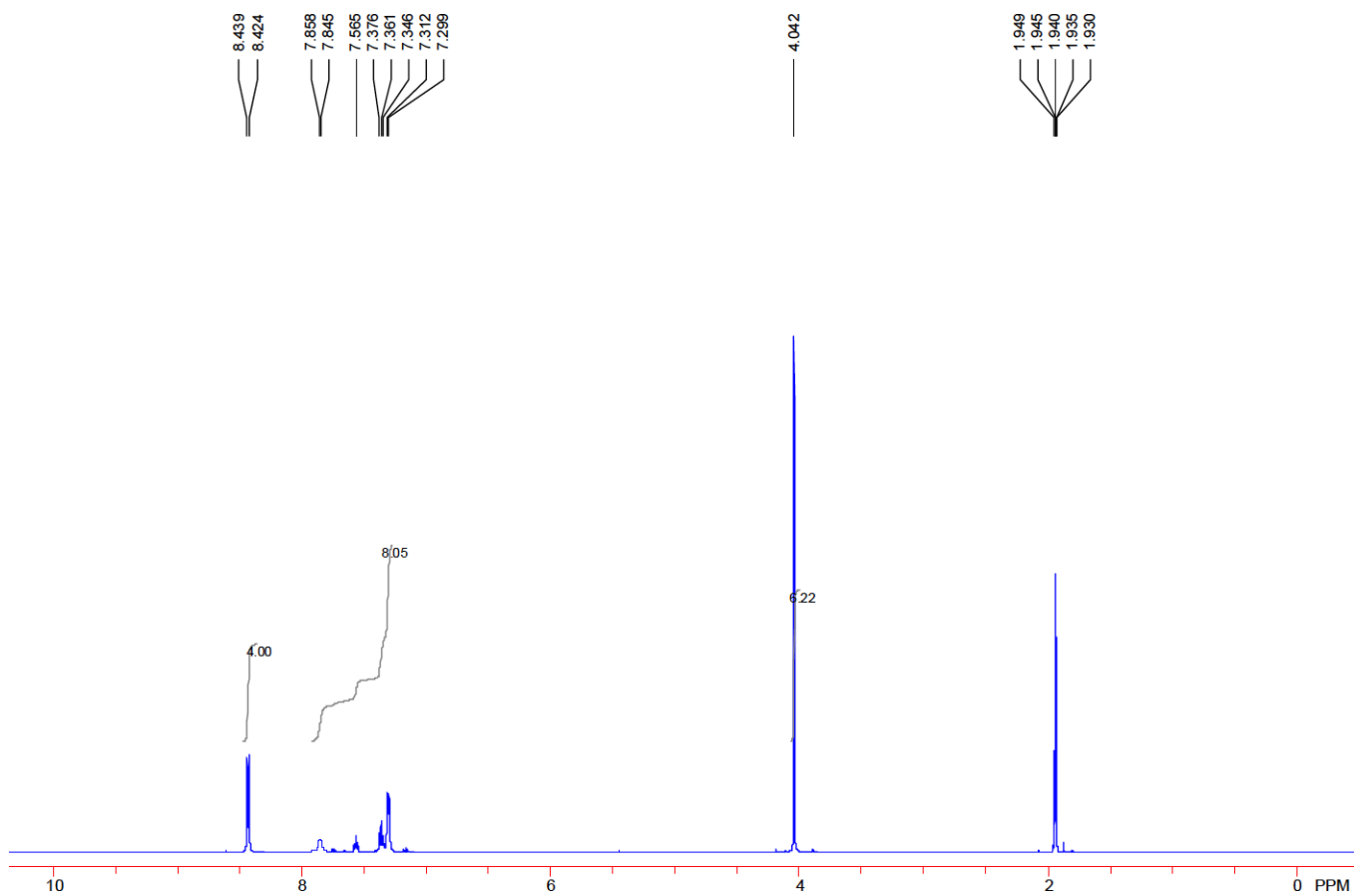


Figure S30: ¹H-NMR spectrum of 1,1'-(phenyl-λ³-iodanediyl)-bis(4-methoxypyridinium)-bis(trifluoromethanesulfonate) (**18**) in CD₃CN.

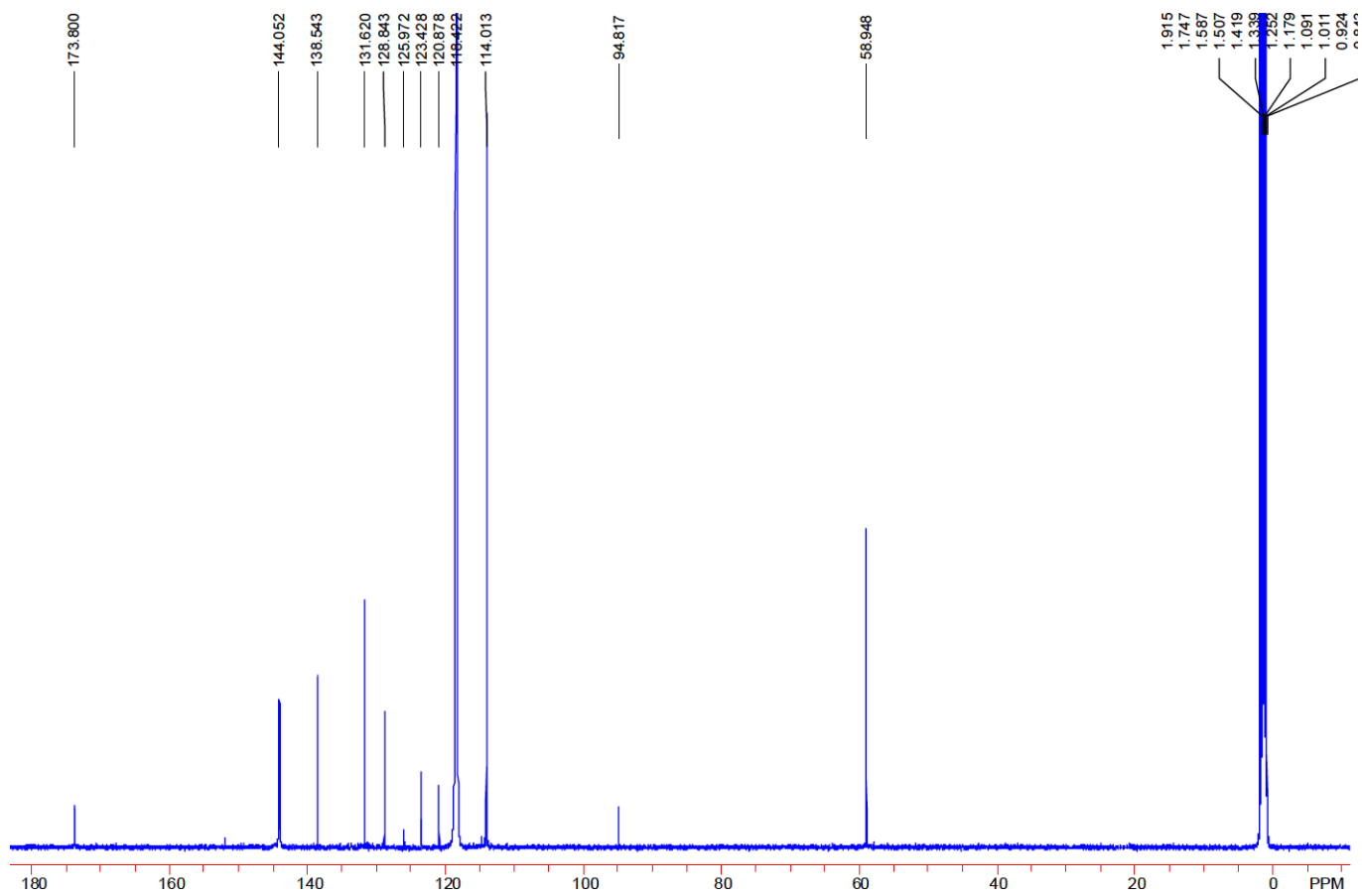


Figure S31: ^{13}C -NMR spectrum of 1,1'-(phenyl- λ^3 -iodanediyl)-bis(4-methoxypyridinium)-bis(trifluoromethanesulfonate) (**18**) in CD_3CN .

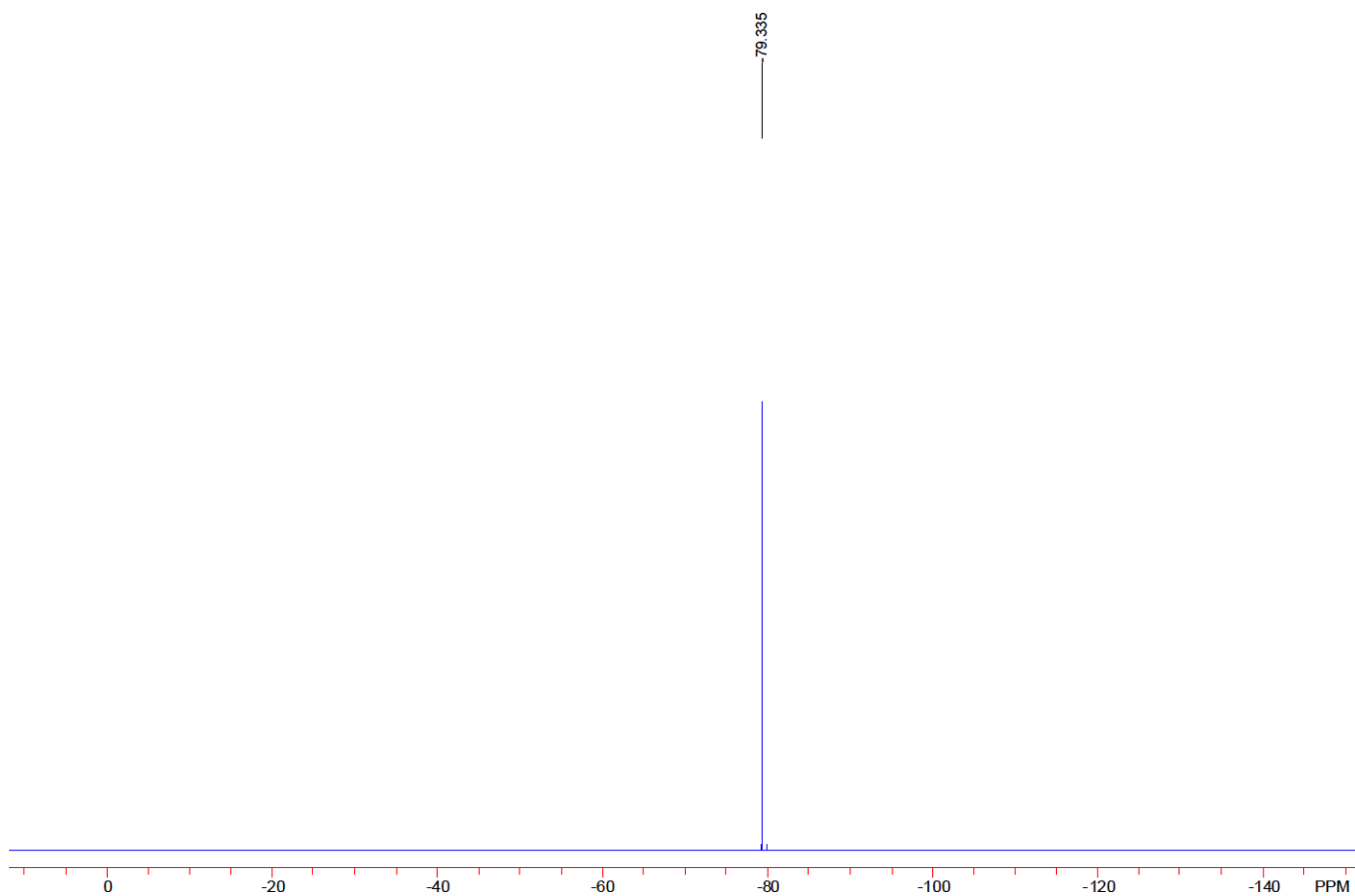


Figure S32: ^{19}F -NMR spectrum of 1,1'-(phenyl- λ^3 -iodanediyl)-bis(4-methoxy pyridinium)-bis(trifluoromethanesulfonate) (**18**) in CD_3CN .

CHAPTER III: Supplementary information

EVALUATION OF [¹¹C]KB631 AS A PET TRACER FOR *IN VIVO* VISUALISATION OF HDAC6 IN B16.F10 MELANOMA

Koen Vermeulen¹, Muneer Ahamed², Kaat Luyten^{1,3} and Guy Bormans¹

¹ Laboratory for Radiopharmaceutical Research, Department of Pharmaceutical and Pharmacological Sciences, KU Leuven, Leuven, Belgium

² Centre for Advanced Imaging, University of Queensland, Brisbane, Australia

³ Switch Laboratory, VIB-KU Leuven Center for Brain & Disease Research, KU Leuven, Leuven, Belgium

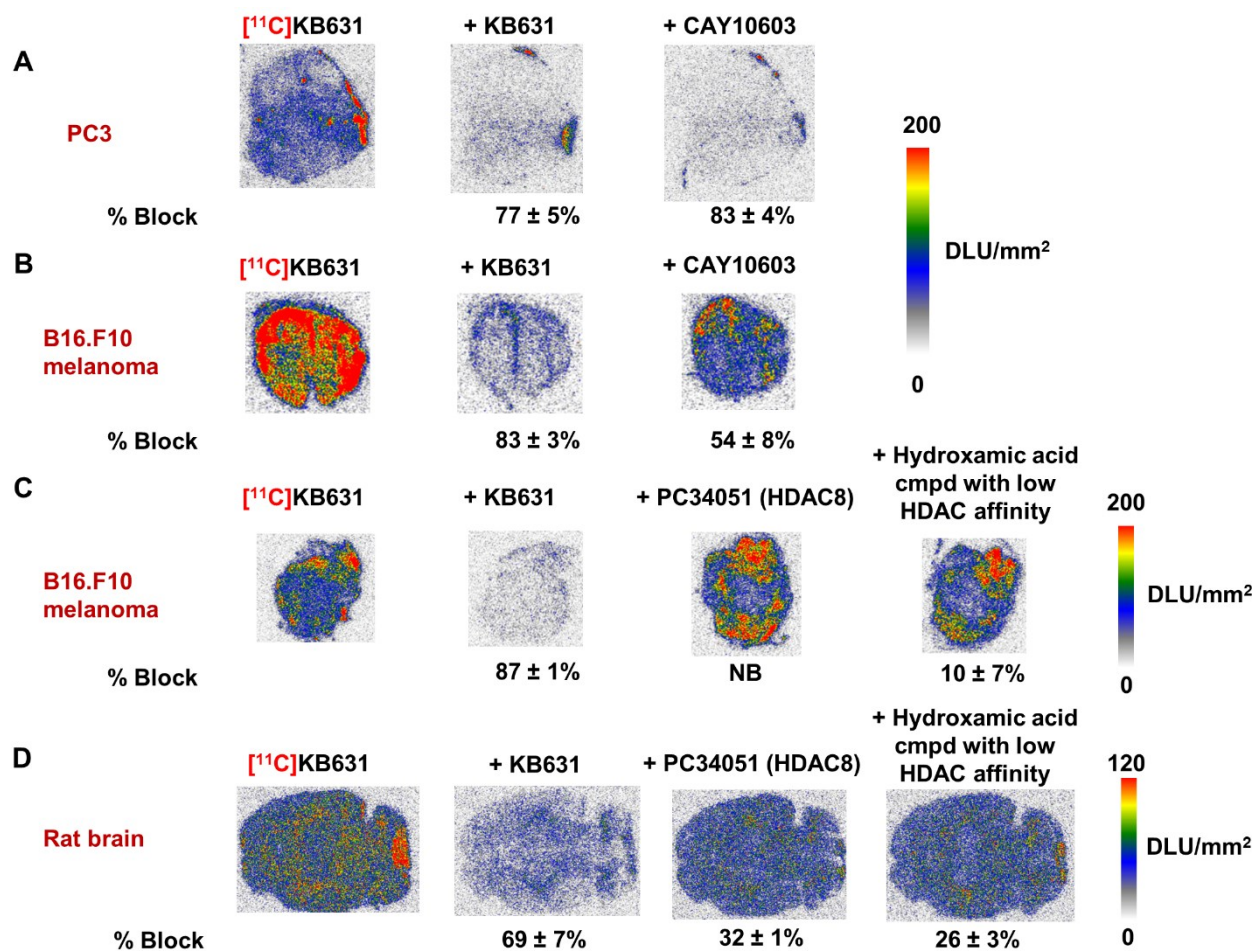


Figure S1: In vitro autoradiography study on different tissue sections. A) PC3 prostate carcinoma **B-C)** B16.F10 melanoma **D)** rat brain. Sections in A-B were incubated with [¹¹C]KB631 (74 kBq/mL) with/without KB631 or CAY10603 (100 μM of blocking agents). Sections in C-D were incubated with [¹¹C]KB631 (74 kBq/mL) with/without KB631, HDAC8 inhibitor PCI34051 or a hydroxamic acid compound with low HDAC affinity (100 μM of blocking agents). Intensity is depicted as DLU/mm². N = 3-4 sections per group. % Block was calculated as (average DLU/mm² in tissue slice in the presence of 100 μM blocker) / (average DLU/mm² in tissue slice, tracer only) and presented as mean ± SD. NB = no block

Table S1: Biodistribution data of [¹¹C]KB631 in male NMRI mice at 2, 10, 30 and 60 min after tracer injection, presented as %ID.

| | %ID ^a | | | |
|-------------------|------------------|------------|------------|------------|
| | 2 min | 10 min | 30 min | 60 min |
| Blood | 6.2 ± 0.3 | 3.7 ± 0.3 | 2.8 ± 0.45 | 1.9 ± 0.6 |
| Bone | 4.5 ± 0.4 | 5.1 ± 0.5 | 3.1 ± 0.3 | 1.8 ± 0.1 |
| Brain | 0.1 ± 0.0 | 0.1 ± 0.0 | 0.1 ± 0.0 | 0.1 ± 0.0 |
| Carcass | 31.5 ± 2.5 | 38.2 ± 1.7 | 26.6 ± 1.4 | 17.0 ± 1.6 |
| Heart | 1.2 ± 0.0 | 0.6 ± 0.1 | 0.4 ± 0.1 | 0.1 ± 0.0 |
| Intestines | 8.9 ± 1.5 | 15.4 ± 0.7 | 31.1 ± 1.9 | 48.6 ± 2.5 |
| Kidneys | 17.4 ± 0.6 | 7.2 ± 1.2 | 5.6 ± 1.0 | 2.0 ± 0.3 |
| Liver | 30.1 ± 4.2 | 25.8 ± 1.2 | 20.2 ± 0.3 | 13.1 ± 2.9 |
| Lungs | 2.5 ± 0.1 | 1.7 ± 0.1 | 1.0 ± 0.1 | 0.7 ± 0.1 |
| Muscle | 27.5 ± 4.1 | 25.3 ± 5.3 | 15.2 ± 1.5 | 6.8 ± 1.3 |
| Pancreas | 1.2 ± 0.2 | 0.8 ± 0.1 | 0.7 ± 0.0 | 0.4 ± 0.1 |
| Spleen | 0.8 ± 0.2 | 0.5 ± 0.1 | 0.2 ± 0.0 | 0.1 ± 0.0 |
| Stomach | 1.2 ± 0.0 | 1.2 ± 0.4 | 2.2 ± 1.2 | 1.2 ± 0.2 |
| Urine | 0.5 ± 0.1 | 5.0 ± 3.1 | 9.3 ± 3.3 | 15.1 ± 3.3 |

%ID = Percentage of injected dose. Data expressed as mean ± SD; n = 3 per time point.

Table S2: Biodistribution data of [¹¹C]KB631 in male NMRI mice 10 min after tracer injection. Mice were pretreated with vehicle, KB631 (10 mg/kg), SAHA (10-100 mg/kg) or Ricolinostat (10-50 mg/kg), presented as %ID.

| | %ID | | | | | |
|-------------------|--------------|------------|------------------|-------------------|--------------------------|--------------------------|
| | Control | KB631 | SAHA 10 mg/kg | SAHA 100 mg/kg | Ricolinostat 10 mg/kg | Ricolinostat 50 mg/kg |
| | Blood | 1.7 ± 0.5 | 6.4 ± 0.4 | 3.9 ± 0.6 | 8.6 ± 2.1 | 4.3 ± 0.2 |
| Bone | 4.6 ± 0.5 | 5.0 ± 0.5 | 4.8 ± 0.7 | 6.3 ± 2.0 | 5.1 ± 0.5 | 7.0 ± 1.0 |
| Brain | 0.1 ± 0.0 | 0.1 ± 0.0 | 0.1 ± 0.0 | 0.1 ± 0.0 | 0.1 ± 0.0 | 0.1 ± 0.0 |
| Carcass | 31.1 ± 1.3 | 41.5 ± 1.4 | 36.0 ± 3.4 | 51.1 ± 17.2 | 33.8 ± 0.8 | 42.7 ± 2.2 |
| Heart | 0.7 ± 0.1 | 0.6 ± 0.1 | 0.7 ± 0.1 | 0.7 ± 0.1 | 0.7 ± 0.2 | 0.8 ± 0.1 |
| Intestines | 16.5 ± 2.1 | 13.2 ± 0.8 | 14.1 ± 2.1 | 8.6 ± 3.2 | 14.6 ± 2.2 | 9.5 ± 0.3 |
| Kidneys | 6.9 ± 0.7 | 14.9 ± 1.6 | 17.2 ± 4.8 | 13.8 ± 5.7 | 6.7 ± 1.0 | 14.7 ± 5.1 |
| Liver | 25.0 ± 4.5 | 19.6 ± 3.1 | 21.0 ± 2.3 | 16.8 ± 6.0 | 26.7 ± 5.8 | 18.9 ± 2.1 |
| Lungs | 1.6 ± 0.0 | 1.6 ± 0.4 | 1.5 ± 0.2 | 1.4 ± 0.8 | 2.3 ± 0.6 | 1.7 ± 0.5 |
| Muscle | 21.7 ± 2.2 | 27.7 ± 4.0 | 29.1 ± 1.2 | 29.1 ± 10.5 | 22.6 ± 3.1 | 31.1 ± 3.6 |
| Pancreas | 1.1 ± 0.2 | 1.0 ± 0.2 | 1.1 ± 0.1 | 1.0 ± 0.4 | 0.9 ± 0.2 | 1.1 ± 0.1 |
| Spleen | 0.3 ± 0.1 | 0.4 ± 0.1 | 0.4 ± 0.1 | 0.3 ± 0.0 | 0.3 ± 0.1 | 0.4 ± 0.1 |
| Stomach | 1.0 ± 0.0 | 1.1 ± 0.2 | 1.0 ± 0.1 | 0.9 ± 0.3 | 1.6 ± 0.4 | 1.2 ± 0.2 |
| Urine | 12.6 ± 1.6 | 2.3 ± 1.0 | 3.4 ± 4.3 | 0.2 ± 0.2 | 8.3 ± 1.4 | 3.6 ± 5.6 |

%ID = Percentage of injected dose. Data expressed as mean ± SD; n = 3 per pre-treatment.

Table S3: Biodistribution data of [¹¹C]KB631 in B16.F10 melanoma inoculated C57BL/6 mice 10 min after tracer injection. Mice were pretreated with vehicle or Ricolinostat (50 mg/kg), presented as %ID.

| | %ID | |
|-------------------|------------|--------------|
| | Control | Ricolinostat |
| Blood | 6.4 ± 0.8 | 13.9 ± 0.9 |
| Bone | 4.8 ± 0.1 | 7.3 ± 2.0 |
| Brain | 0.2 ± 0.0 | 0.2 ± 0.0 |
| Carcass | 36.3 ± 0.6 | 41.6 ± 5.3 |
| Heart | 0.8 ± 0.1 | 0.7 ± 0.1 |
| Intestines | 15.1 ± 0.3 | 12.3 ± 1.6 |
| Kidneys | 12.0 ± 0.7 | 8.4 ± 1.9 |
| Liver | 23.9 ± 1.9 | 19.2 ± 3.1 |
| Lungs | 1.8 ± 0.2 | 2.0 ± 0.3 |
| Muscle | 20.4 ± 1.2 | 27.3 ± 0.3 |
| Pancreas | 1.1 ± 0.1 | 1.2 ± 0.2 |
| Spleen | 0.5 ± 0.0 | 0.6 ± 0.0 |
| Stomach | 0.9 ± 0.2 | 1.0 ± 0.1 |
| Tumour | 1.7 ± 0.3 | 3.9 ± 1.1 |
| Urine | 1.9 ± 2.4 | 3.4 ± 5.6 |

%ID = Percentage of injected dose. Data expressed as mean ± SD; n = 3 per pre-treatment.

CHAPTER IV: Supplementary information

EVALUATION OF [¹¹C]NMS-E973 AS A PET TRACER FOR *IN VIVO* VISUALISATION OF HSP90

Koen Vermeulen^{1*}, Evelyne Naus^{2*}, Muneer Ahamed³, Bala Attili¹, Maxime Siemons^{1,2}, Kaat Luyten^{1,2}, Sofie Celen¹, Joost Schymkowitz², Frederic Rousseau² and Guy Bormans¹

¹ Laboratory for Radiopharmaceutical Research, Department of Pharmaceutical and Pharmacological Sciences, KU Leuven, Leuven, Belgium

² Switch Laboratory, VIB-KU Leuven Center for Brain & Disease Research, KU Leuven, Leuven, Belgium

³ Centre for Advanced Imaging, University of Queensland, Brisbane, Australia

*These authors contributed equally to this manuscript.

Chemical synthesis of precursor compound, 7

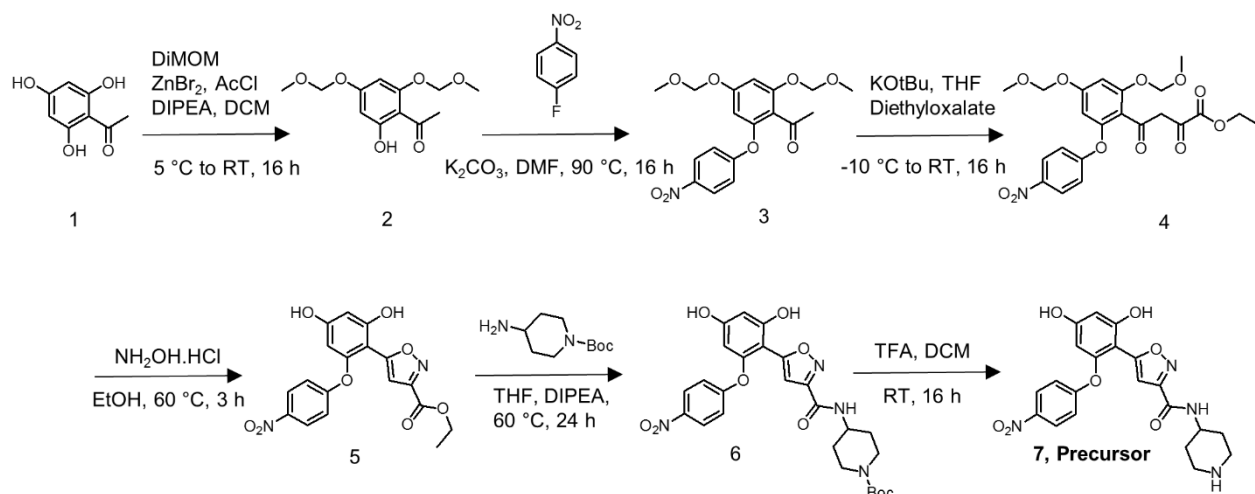


Figure S1: Synthesis of precursor compound **7**.

1-[2-hydroxy-4,6-bis(methoxymethoxy)phenyl]ethanone (2). To a stirred solution of dimethoxymethane (2.64 ml, 29.8 mmol) and zinc bromide (29.28 mg, 0.13 mmol) in DCM (23,2 mL), acetyl chloride (2.12 mL, 29.8 mmol) was added dropwise during 30 min maintaining the temperature below 30 °C. After stirring for 3 h at room temperature, the solution was diluted with DCM (48 mL), then cooled to 5 °C before the portion wise addition of 1-(2,4,6-trihydroxyphenyl)ethanone (**1**), 2.00 g, 11.89 mmol) followed by the dropwise addition of *N,N*-diisopropylethylamine (8.32 mL, 47.6 mmol). After 1 h the ice bath was removed and the temperature was allowed to rise to RT. The resulting solution was stirred for 16 h, and washed with NH₄Cl saturated solution, followed by washing with 10% citric acid solution. After drying over MgSO₄, the solvent was removed and purification was performed with column chromatography to yield (**2**) (Yield: 0.75 g, 37%) *Colorless oil*, ¹H NMR (CDCl₃-d): δ 2.66 (s, 3H, CH₃), 3.48 (s, 3H, CH₃), 3.52 (s, 3H, CH₃), 5.17 (s, 2H, CH₂), 5.26 (s, 2H, CH₂), 6.23-6.28 (m, 2H, Ar). ¹³C NMR (CDCl₃): δ 33.2, 56.7, 56.9, 94.2 (2C), 94.7, 97.4, 107.2, 160.6, 163.7, 167.0, 200.4. HRMS (ESI) calculated for C₁₂H₁₇O₆ [M+H]⁺: 257.1020. Found: 257.1023

1-[2,4-Bis(methoxymethoxy)-6-(4-nitrophenoxy-phenyl)]ethanone (3). To a stirred solution of (**2**) (745 mg, 2.91 mmol) in DMF (6 mL) 4-nitro-1-fluorobenzene (0.34 mL, 3.20 mmol) was added, followed by K₂CO₃ (803 mg, 5.82 mmol). After stirring for 15 min at room temperature, the resulting suspension was heated for 16 h at 90 °C. After cooling, the dark solution was diluted with EtOAc (20 mL) and thoroughly washed with 10% citric acid solution and brine and dried over MgSO₄. The solvent was removed and the residue was purified by column chromatography to yield (**3**). (Yield: 0.43 g, 58%). *Yellow powder*, ¹H NMR (CDCl₃): δ 2.43 (s, 3H, CH₃), 3.44 (s, 3H, CH₃), 3.49 (s, 3H, CH₃),

5.11 (s, 2H, CH₂), 5.20 (s, 2H, CH₂), 6.35 (s, 1H, Ar), 6.73 (s, 1H, Ar), 7.00 (d, 2H, *J* = 9.2 Hz, Ar), 8.18 (d, 2H *J* = 9.2 Hz, Ar). ¹³C NMR (CDCl₃-*d*): δ 33.0, 57.0, 57.2, 95.1, 95.6, 101.3, 102.9, 117.8, 120.0, 126.6, 143.6, 153.3, 157.1, 160.6, 163.6, 200.0. HRMS (ESI) calculated for C₁₈H₁₉NO₈ [M+H]⁺: 378.1184. Found: 378.1179.

Ethyl 5-[2,4-bis(methoxymethoxy)-6-(4-nitrophenoxy)phenyl]-2,4-dioxobutanoate (4). To a stirred solution of sodium *tert*-butoxide (0.284 g, 2.51 mmol) in THF (8 mL) at -10 °C, was added diethyl oxalate (0.5 mL, 3.42 mmol) in 2 mL of precooled THF. After 30 min a solution of (3) (430 mg, 1.14 mmol) in THF (4 mL) was added drop wise. The reaction mixture was stirred for 1 h at -10 °C and then further 16 h at room temperature. The solution was poured into a 10% citric acid solution (30 mL) and thoroughly extracted with EtOAc. After washing with brine and drying over MgSO₄, the combined organic fractions were evaporated to provide a yellow crude residue. Purification using column chromatography yielded (4). (Yield: 98%, proceeded to the next step without further characterization)

Ethyl 5-[2,4-bis(methoxymethoxy)-6-(4-nitrophenoxy)phenyl]-isoxazole-3-carboxylate (5). To a stirred solution of (4) (0.42 g, 0.88 mmol) in EtOH (12 mL), hydroxylamine hydrochloride (2.67 mg, 4.02 mmol) was added. After stirring for 3 h at 60 °C, the solvent was evaporated, saturated NaHCO₃ (30 mL) was added and the suspension was taken up in DCM (30 mL) and thoroughly washed with water and dried over MgSO₄. The solvent was removed by evaporation and purification using column chromatography was performed to afford (5). (Yield: 0.15 g, 35%) *Yellow oil*, ¹H NMR (MeOD-*d*₄): δ 1.30-1.37 (m, 3H, CH₃), 4.32-4.36 (m, 2H, CH₂), 6.11 (s, 1H, Ar), 6.38 (s, 1H, Ar), 6.87 (s, 1H, Ar), 7.04 (d, 2H *J* = 8.8 Hz, Ar), 8.16 (d, 2H *J* = 8.8 Hz, Ar). ¹³C NMR (MeOD-*d*₄): δ 13.6, 62.3, 100.6, 101.2, 104.7, 117.2, 120.1, 126.2, 143.4, 154.8, 156.4, 159.2, 160.7, 162.2, 163.7, 167.4. HRMS (ESI) calculated for C₁₈H₁₅N₂O₈ [M+H]⁺: 387.0822. Found: 387.0841.

***Tert*-butyl-4-[[[5-[2,4-bis(methoxymethoxy)-6-(4-nitrophenoxy)phenyl]-isoxazole-3-yl]carbonyl]amino]piperidin-1-carboxylate (6).** (5) (149 mg, 0.3859 mmol) and *tert*-butyl 4-aminopiperidine-1-carboxylate (386 mg, 1.93 mmol) were dissolved in THF (12 mL). *N,N*-diisopropylethylamine (1.34 mL, 0.77 mmol) was added to the mixture. The reaction mixture was stirred at 60 °C for 24 h. After cooling to room temperature, the solvent was removed. The residue was purified by column chromatography to afford (6). *Brownish oil*, ¹H NMR (MeOD-*d*₄): δ 1.13-1.20 (m, 4H, CH₂), 1.40 (s, 9H, 3CH₃), 3.93-4.01 (m, 5H, CH₂ & CH), 6.05 (s, 1H, Ar), 6.31 (s, 1H, Ar), 6.79 (s, 1H, Ar), 6.95 (d, 2H *J* = 8.6 Hz, Ar), 8.09 (d, 2H *J* = 8.6 Hz, Ar). ¹³C NMR (MeOD-*d*₄): δ 13.8, 20.2, 28.0, 31.6, 80.5, 100.7, 100.9, 101.2, 103.7, 117.1, 126.2, 143.3, 154.7, 155.7, 158.7, 159.1, 160.3, 162.0, 163.8, 166.8, 172.3. HRMS (ESI) calculated for C₂₆H₂₉N₄O₉ [M+H]⁺: 541.1929. Found: 541.1914.

5-[2,4-Dihydroxy-6-(4-nitrophenoxy) phenyl]-N-(piperidin-4-yl)-isoxazole-3-carboxamide (7). To a stirred solution of **(6)** (50 mg) in DCM (5 mL) was added TFA (3 eq), the reaction mixture was stirred for 16 h and monitored by LC-MS. After completion, the reaction mixture was diluted with DCM (10 mL) and washed with 0.1 M NaOH and saturated NaHCO₃. Purification over a short pad of silica gel yielded **(7)**. *Pale yellow oil*, ¹H NMR (DMSO-*d*₆): δ 1.32-1.38 (m, 4H), 2.57-3.59 (m, 2H), 2.91-2.93 (m, 2H), 3.98-4.01 (m, 1H), 6.07 (s, 1H), 6.33 (s, 1H), 6.80 (s, 1H), 6.96-6.98 (m, 2H), 8.12-8.14 (m, 2H). ¹³C NMR (DMSO-*d*₆): δ 27.8, 42.3, 44.0, 99.5, 100.4, 100.5, 103.3, 116.8, 126.1, 142.1, 153.4, 158.1, 158.3, 158.3, 161.2, 162.8, 165.4. HRMS (ESI) calculated for C₂₁H₂₁N₄O₇ [M + H⁺]: 441.1404. Found: 441.1410.

Immunofluorescent staining of B16.F10 melanoma cells and high-content screening

Cells were plated in a 96-well plate (Greiner) at a density of 8000-10000 cells/well. At day 1, cells were treated with vehicle (DMSO; 0.001% final concentration), or with a compound (NMS-E973 or Ganetespib) at indicated final concentration (250 nM or 500 nM) for 16 hours. At day 2 cells were washed with PBS and fixed with 4% paraformaldehyde (Thermo Scientific, 16% PFA diluted in PBS) for 30 minutes and were either permeabilised or not by adding 0.2% Triton X100 to blocking buffer (1% Bovine Serum Albumine (BSA) in PBS) for 60 minutes. Primary antibodies were added to the cells in blocking buffer at a dilution of 1:500 (Anti-HSP90, AC88, Abcam) and incubated overnight at 4 °C while shaking gently. Cells were washed 3 times for 5 minutes in PBS and subsequently incubated with DAPI (0.1 µg/ml and/or secondary antibody (1:1000 goat-anti mouse alexa-594; PROMEGA) in blocking buffer for 60 minutes. Imaging was performed on the IN Cell Analyser 2000 (GE Healthcare). The IN Cell Developer package (v1.9.2) allows visualization, imaging, and quantification of staining intensity and quantification of inclusions in cells following immunofluorescent staining.

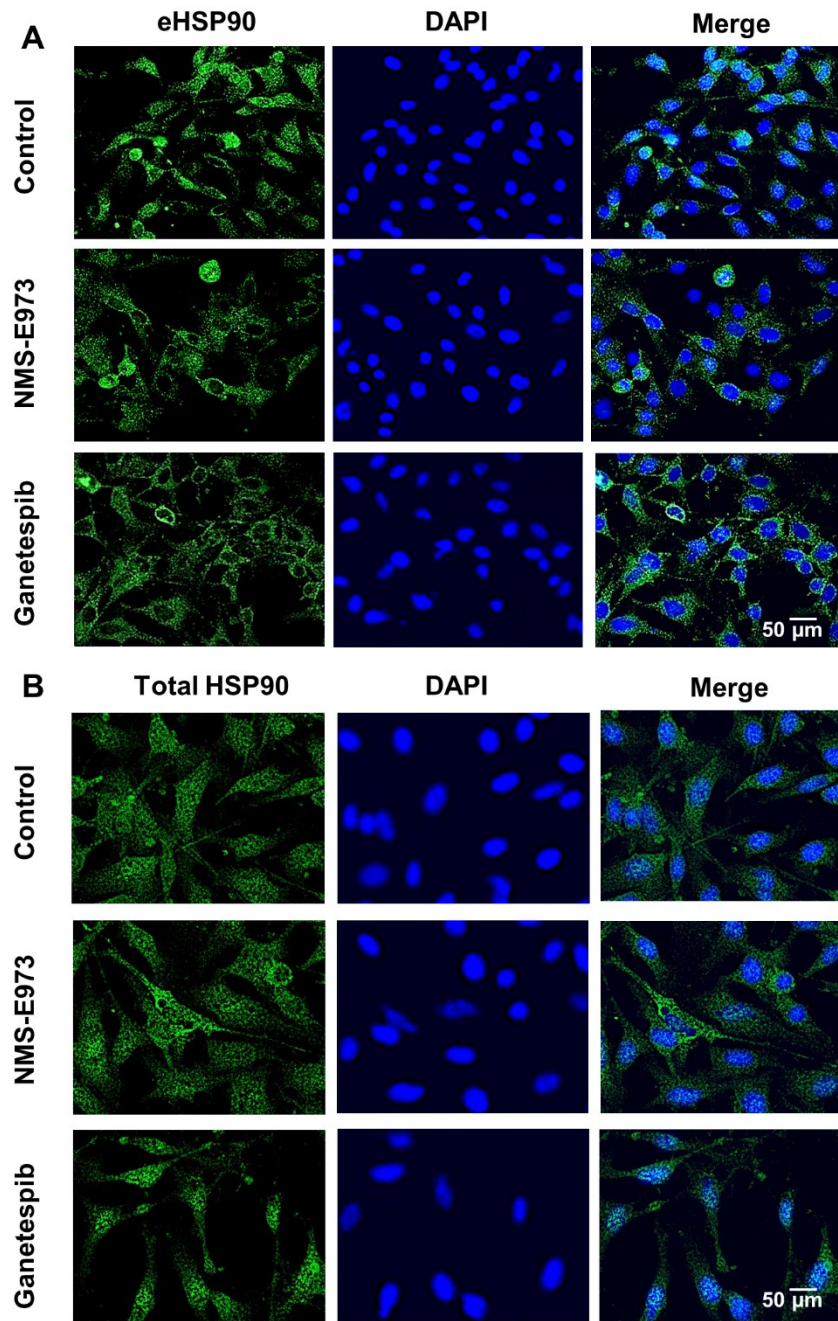


Figure S2: Immunofluorescent staining of eHSP90 and HSP90 of the B16.F10 melanoma cells. (A) Extracellular staining of HSP90 shows membrane staining that excludes the nucleus. FITC-Staining of HSP90 (left, Green), nuclear staining by DAPI (Middle, Blue) and the overlay (Right). Treatment with either Ganetespiib or NMS-E973, both at 500 nM for 16 hours, shows no visual difference in phenotype (scale bar 50 μ m). **(B)** Total staining of HSP90 after permeabilisation, shows homogeneous cellular staining. FITC-Staining of HSP90 (Left, Green), nuclear staining by DAPI (Middle, Blue) and the overlay (Right). Treatments with either Ganetespiib or NMS-E973, both at 500 nM for 16 hours, shows no visual difference in phenotype (scale bar 50 μ m).

SDS/Western blot analysis on B16.F10 melanoma cells

Analysis of protein expression was carried out on all cell lines plated at a density of 250,000 cells in a 6-well plate at day 0. At day 1, cells were treated with vehicle (DMSO; 0.001% final concentration), or with 250 nM or 500 nM of NMS-E973 or Ganetespib for 16 hours. At day 2, cells were washed with PBS and lysed in 200 μ l NP40 lysis buffer (150 mM NaCl, 50 mM Tris-HCl pH 8, 1% IGEPAL(NP40), containing a 1X PBS dissolved complete protease inhibitor cocktail (Roche) and 1U/ μ l Universal Nuclease (Pierce) for 30 minutes on ice. Lysates were subjected to regular SDS/Western blot analysis. Antibodies for detection include anti-Cyclin-dependent kinase 1 (CDK1) (Santa Cruz Biotechnology) and anti-GAPDH (6C5; Santa Cruz Biotechnology). Secondary HRP-linked antibodies were used (PROMEGA). Quantification is done by densitometry using the ImageJ software package. Normalization is corrected to GAPDH levels of the input.

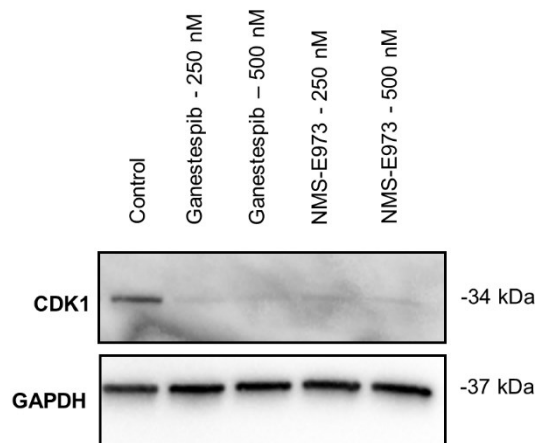


Figure S3: Effect of NMS-E973 and Ganetespib treatment on client protein CDK1 expression. Representative Western blot of decreased CDK1 expression after treatment shows that HSP90 is effectively inhibited by different concentrations of Ganetespib and NMS-E973.

QC chromatogram of [¹¹C]NMS-E973

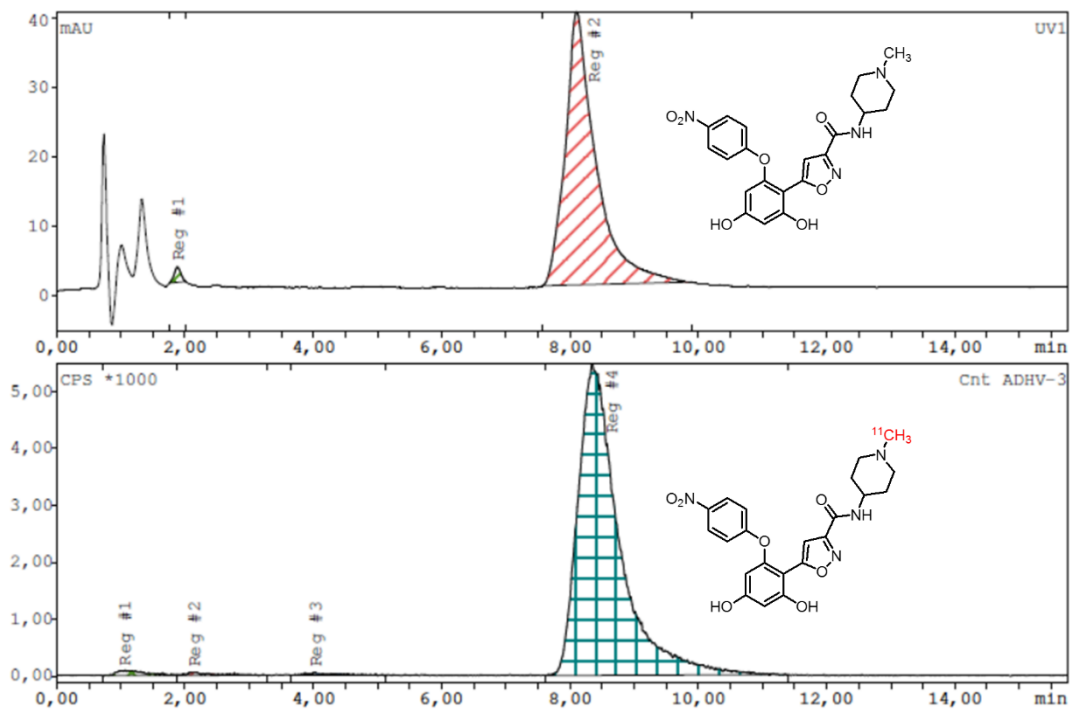


Figure S4: QC chromatogram of [¹¹C]NMS-E973 spiked with authentic reference compound NMS-E973 on an X-bridge RP-C₁₈ column (100 x 3 mm 3.5 μm) (upper channel UV 254 nm, lower channel radioactivity)

Confirmation of N-methylation

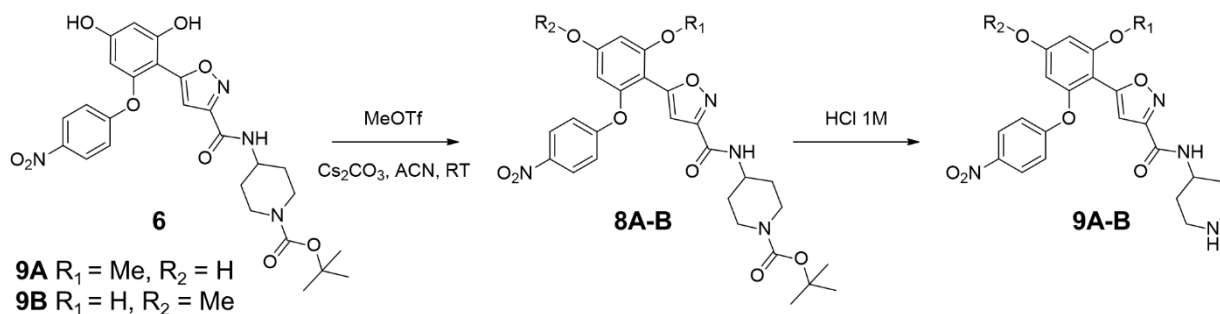


Figure S5: Synthesis of O-alkylated compound starting from (**6**) which is treated with Methyl triflate (MeOTf) under alkaline conditions to form **8A-B**, which is treated with 1 M HCl to remove the BOC-protection group to yield compounds **9A-B**.

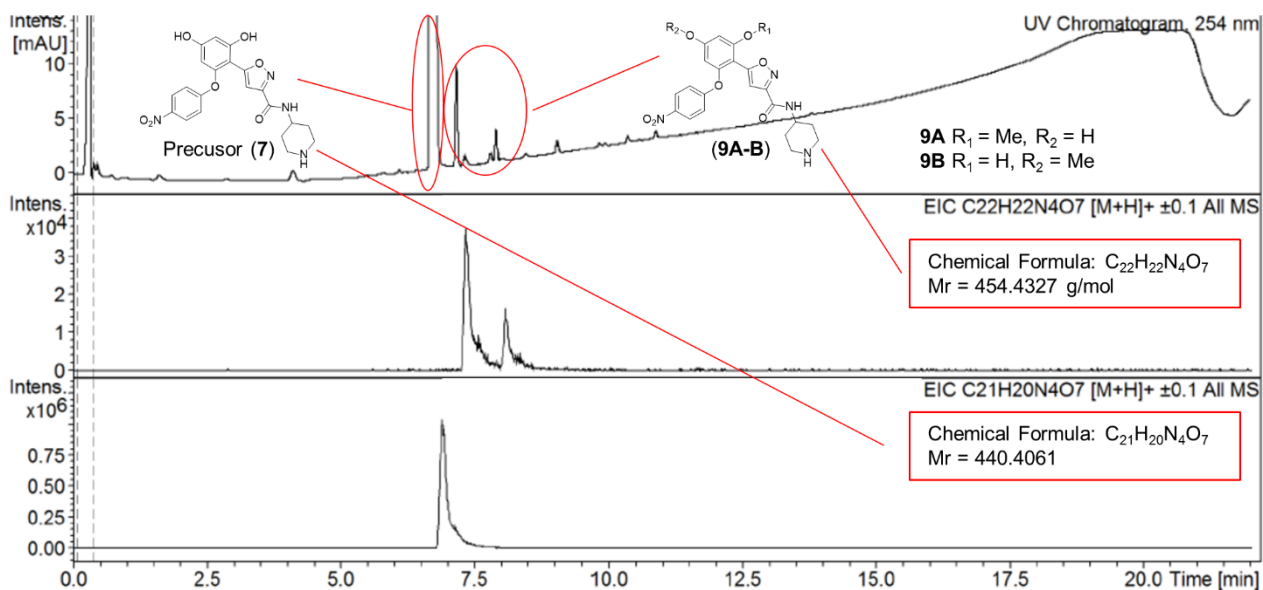


Figure S6: LC-MS-chromatograms of the reaction mixture yielding compound **9A-B**. Extracted ion chromatograms (EIC 454.4 ± 0.1 Da, Rt 7.7 min and 8.5 min) indicate formation of 2 O-methylated compounds **9A-B** that are present besides excess of deprotected precursor compound **7** (EIC 440.4 ± 0.1 Da, Rt 6.9 min). Samples were run on a LC/HRMS system, described in the materials and method section, over an Acquity UPLC BEH C₁₈ column (1.7 μm, 2.1 mm x 150 mm, Waters), using a 22 min gradient containing H₂O + 0.1% HCOOH and ACN + 0.1% HCOOH (95/5 to 5/95) with a flow rate of 0.3 mL/min.

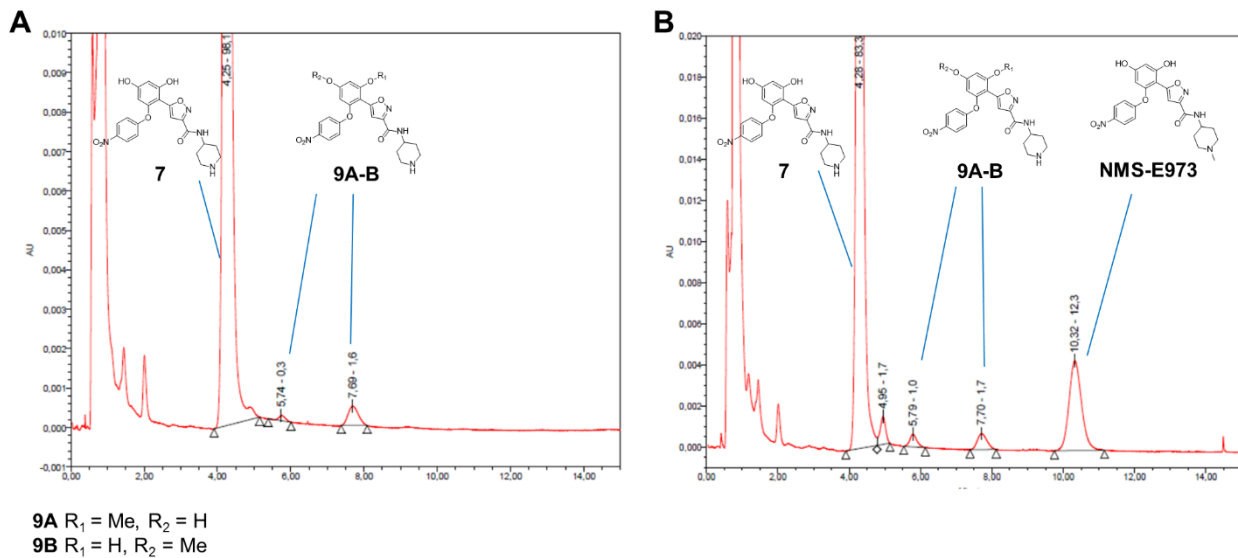


Figure S7: QC HPLC analysis (UV 254 nm) – chromatograms. **A)** Injection of crude reaction mixture, containing precursor compound (**7**) (Rt 4.2 min) and **O-methylated compounds 9A-B** (Rt 5.7 min and 7.7 min). **B)** Coinjection of crude reaction mixture with NMS-E973. Precursor (**7**) (Rt 4.2 min), **O-methylated products 9A-B** (Rt 5.8 min and 7.7) and NMS-E973 (Rt 10.3 min) show a clear difference in retention time. UV detection was performed at 254 nm.

Plasma radiometabolite study and biodistribution studies

Table S1: Gradient mixture and flow rate used at given time points for radiometabolite study of [¹¹C]NMS-E973 with a Chromolith RP C₁₈ column.

| Time (min) | A (ACN) (%) | B (NaOAc 0.05 M pH 5.5) (%) | Flow (mL/min) |
|------------|-------------|-----------------------------|---------------|
| 0 | 1 | 99 | 0.5 |
| 4 | 1 | 99 | 0.5 |
| 4.1 | 1 | 99 | 1.0 |
| 9 | 90 | 10 | 1.0 |
| 12 | 90 | 10 | 1.0 |
| 12.1 | 90 | 10 | 0.5 |
| 15 | 1 | 99 | 0.5 |

Table S2: Biodistribution data of [¹¹C]NMS-E973 in female Wistar rats at 2, 10, 30 and 60 min after tracer injection.

| %ID ^a | | | | |
|-------------------|------------|------------|------------|------------|
| | 2 min | 10 min | 30 min | 60 min |
| Blood | 17.6 ± 1.5 | 9.7 ± 1.1 | 5.3 ± 1.1 | 2.6 ± 0.8 |
| Bone | 5.7 ± 1.0 | 3.7 ± 0.3 | 3.8 ± 0.2 | 1.6 ± 0.1 |
| Brain | 0.1 ± 0.0 | 0.0 ± 0.0 | 0.0 ± 0.0 | 0.0 ± 0.0 |
| Carcass | 27.3 ± 1.9 | 23.2 ± 0.7 | 23.7 ± 1.0 | 17.2 ± 2.6 |
| Heart | 0.6 ± 0.1 | 0.4 ± 0.1 | 0.5 ± 0.0 | 0.3 ± 0.0 |
| Intestines | 9.3 ± 1.0 | 25.8 ± 2.9 | 41.8 ± 7.6 | 40.6 ± 4.2 |
| Kidneys | 14.8 ± 1.2 | 9.6 ± 1.4 | 5.2 ± 0.4 | 2.1 ± 0.4 |
| Liver | 33.8 ± 3.7 | 25.9 ± 3.4 | 12.5 ± 4.0 | 11.3 ± 0.7 |
| Lungs | 1.2 ± 0.3 | 1.0 ± 0.3 | 0.6 ± 0.1 | 0.6 ± 0.1 |
| Muscle | 13.4 ± 0.7 | 12.7 ± 0.2 | 14.5 ± 1.5 | 10.2 ± 0.8 |
| Pancreas | 0.5 ± 0.1 | 0.7 ± 0.2 | 0.6 ± 0.1 | 0.6 ± 0.2 |
| Spleen | 0.6 ± 0.1 | 0.4 ± 0.0 | 0.4 ± 0.0 | 0.3 ± 0.0 |
| Stomach | 1.1 ± 1.1 | 3.9 ± 0.6 | 6.1 ± 5.1 | 14.0 ± 5.2 |
| Urine | 0.0 ± 0.0 | 2.7 ± 1.0 | 4.8 ± 1.2 | 11.3 ± 1.4 |
| SUV ^b | | | | |
| | 2 min | 10 min | 30 min | 60 min |
| Blood | 2.5 ± 0.2 | 1.4 ± 0.2 | 0.8 ± 0.2 | 0.4 ± 0.1 |
| Bone | 0.5 ± 0.1 | 0.3 ± 0.0 | 0.3 ± 0.0 | 0.1 ± 0.0 |
| Brain | 0.1 ± 0.0 | 0.0 ± 0.0 | 0.0 ± 0.0 | 0.0 ± 0.0 |
| Heart | 1.6 ± 0.1 | 1.3 ± 0.1 | 1.3 ± 0.1 | 1.1 ± 0.1 |
| Kidneys | 17.3 ± 0.6 | 12.5 ± 1.6 | 5.8 ± 0.5 | 3.0 ± 0.7 |
| Liver | 9.3 ± 0.3 | 7.9 ± 1.1 | 3.3 ± 1.1 | 3.5 ± 0.5 |
| Lungs | 1.8 ± 0.3 | 1.4 ± 0.1 | 1.2 ± 0.1 | 1.0 ± 0.1 |
| Muscle | 0.3 ± 0.0 | 0.3 ± 0.0 | 0.4 ± 0.0 | 0.3 ± 0.0 |
| Pancreas | 1.6 ± 0.3 | 1.4 ± 0.1 | 1.4 ± 0.1 | 1.3 ± 0.2 |
| Spleen | 2.3 ± 0.2 | 2.2 ± 0.1 | 1.4 ± 0.1 | 1.3 ± 0.1 |

^a Percentage of injected dose calculated as cpm in organ/total cpm recovered) x 100. ^b SUV calculated as (radioactivity in cpm in organ/weight of organ in grams)/(total cpm recovered/body weight). Data expressed as mean ± SD; n = 3 per time point.

Table S3: Biodistribution data of [¹¹C]NMS-E973 in male NMRI-mice at 2, 10, 30 and 60 min after tracer injection.

| %ID ^a | | | | |
|-------------------|------------|------------|------------|------------|
| | 2 min | 10 min | 30 min | 60 min |
| Blood | 8.8 ± 0.6 | 4.7 ± 0.9 | 2.1 ± 0.6 | 1.3 ± 0.1 |
| Bone | 2.8 ± 0.3 | 2.0 ± 0.3 | 1.8 ± 0.2 | 1.2 ± 0.1 |
| Brain | 0.1 ± 0.0 | 0.0 ± 0.0 | 0.1 ± 0.0 | 0.0 ± 0.0 |
| Carcass | 15.6 ± 0.7 | 15.5 ± 1.1 | 14.8 ± 1.3 | 10.9 ± 2.3 |
| Heart | 0.4 ± 0.1 | 0.4 ± 0.1 | 0.3 ± 0.0 | 0.2 ± 0.0 |
| Intestines | 12.2 ± 1.5 | 35.7 ± 0.4 | 47.0 ± 0.7 | 56.2 ± 6.2 |
| Kidneys | 14.4 ± 0.6 | 7.8 ± 1.1 | 5.2 ± 1.9 | 2.1 ± 0.4 |
| Liver | 48.5 ± 1.8 | 24.1 ± 3.9 | 11.0 ± 2.3 | 7.9 ± 1.5 |
| Lungs | 0.7 ± 0.1 | 0.5 ± 0.1 | 0.5 ± 0.2 | 0.3 ± 0.1 |
| Muscle | 9.8 ± 0.5 | 8.6 ± 1.0 | 8.7 ± 1.2 | 5.3 ± 0.4 |
| Pancreas | 0.5 ± 0.1 | 0.5 ± 0.1 | 0.7 ± 0.1 | 0.3 ± 0.0 |
| Spleen | 0.2 ± 0.1 | 0.2 ± 0.1 | 0.1 ± 0.0 | 0.1 ± 0.0 |
| Stomach | 0.4 ± 0.0 | 1.1 ± 1.1 | 0.7 ± 0.4 | 0.4 ± 0.2 |
| Testes | 0.0 ± 0.0 | 0.1 ± 0.1 | 0.1 ± 0.0 | 0.0 ± 0.0 |
| Urine | 0.2 ± 0.2 | 10.6 ± 2.7 | 16.7 ± 2.4 | 20.3 ± 3.5 |
| SUV ^b | | | | |
| | 2 min | 10 min | 30 min | 60 min |
| Blood | 1.3 ± 0.1 | 0.7 ± 0.1 | 0.3 ± 0.1 | 0.2 ± 0.0 |
| Bone | 0.2 ± 0.0 | 0.2 ± 0.0 | 0.1 ± 0.0 | 0.1 ± 0.0 |
| Brain | 0.1 ± 0.0 | 0.0 ± 0.0 | 0.0 ± 0.0 | 0.0 ± 0.0 |
| Heart | 0.8 ± 0.1 | 0.7 ± 0.1 | 0.6 ± 0.1 | 0.5 ± 0.1 |
| Kidneys | 7.7 ± 0.8 | 4.4 ± 0.2 | 2.7 ± 1.1 | 1.1 ± 0.2 |
| Liver | 8.6 ± 0.4 | 4.4 ± 0.7 | 2.1 ± 0.1 | 1.4 ± 0.3 |
| Lungs | 0.8 ± 0.1 | 0.8 ± 0.2 | 0.5 ± 0.1 | 0.5 ± 0.2 |
| Muscle | 0.2 ± 0.0 | 0.2 ± 0.0 | 0.2 ± 0.0 | 0.1 ± 0.0 |
| Pancreas | 0.6 ± 0.1 | 0.7 ± 0.1 | 0.7 ± 0.0 | 0.5 ± 0.1 |
| Spleen | 0.6 ± 0.1 | 0.7 ± 0.2 | 0.4 ± 0.1 | 0.3 ± 0.1 |
| Testes | 0.1 ± 0.0 | 0.2 ± 0.1 | 0.1 ± 0.1 | ± 0.0 |

^a Percentage of injected dose calculated as (cpm in organ/total cpm recovered) x 100. ^b SUV calculated as (radioactivity in cpm in organ/weight of organ in grams)/(total cpm recovered/body weight). Data expressed as mean ± SD; n = 3 per time point.

Table S4: Biodistribution data of [¹¹C]NMS-E973 in male NMRI-mice pretreated with vehicle, NMS-E973 (25mg/kg) or PU-H71 (50 mg/kg) at 10 min after tracer injection.

| %ID^a 10 min p.i. | | | |
|------------------------------------|----------------|------------------------------|----------------------------|
| | Control | NMS-E973 pretreatment | PU-H71 pretreatment |
| Blood | 4.9 ± 0.8 | 2.5 ± 0.2 | 6.3 ± 0.2 |
| Bone | 2.6 ± 0.0 | 2.6 ± 0.5 | 3.1 ± 0.5 |
| Brain | 0.1 ± 0.0 | 0.0 ± 0.0 | 0.1 ± 0.0 |
| Carcass | 20.0 ± 1.8 | 17.1 ± 2.2 | 28.0 ± 1.5 |
| Heart | 0.5 ± 0.2 | 0.3 ± 0.0 | 0.5 ± 0.1 |
| Intestines | 27.0 ± 0.5 | 33.3 ± 4.0 | 20.6 ± 0.6 |
| Kidneys | 12.8 ± 10.0 | 5.3 ± 0.4 | 17.2 ± 6.4 |
| Liver | 23.8 ± 2.3 | 24.6 ± 2.6 | 18.4 ± 2.6 |
| Lungs | 0.7 ± 0.1 | 0.5 ± 0.1 | 0.8 ± 0.2 |
| Muscle | 11.7 ± 0.4 | 10.2 ± 1.8 | 14.6 ± 3.1 |
| Pancreas | 0.5 ± 0.1 | 0.5 ± 0.0 | 0.5 ± 0.1 |
| Spleen | 0.1 ± 0.1 | 0.1 ± 0.0 | 0.2 ± 0.0 |
| Stomach | 0.4 ± 0.0 | 0.4 ± 0.1 | 0.5 ± 0.0 |
| Testes | 0.1 ± 0.0 | 0.1 ± 0.0 | 0.1 ± 0.0 |
| Urine | 10.8 ± 15.1 | 15.4 ± 1.7 | 7.2 ± 7.4 |
| SUV^b 10 min p.i. | | | |
| | Control | NMS-E973 pretreatment | PU-H71 pretreatment |
| Blood | 0.7 ± 0.1 | 0.4 ± 0.0 | 0.9 ± 0.0 |
| Bone | 0.2 ± 0.0 | 0.2 ± 0.0 | 0.3 ± 0.0 |
| Brain | 0.1 ± 0.0 | 0.0 ± 0.0 | 0.1 ± 0.0 |
| Heart | 1.0 ± 0.2 | 0.8 ± 0.0 | 1.0 ± 0.1 |
| Kidneys | 7.0 ± 4.8 | 3.6 ± 0.2 | 9.2 ± 3.2 |
| Liver | 3.8 ± 0.2 | 4.3 ± 0.7 | 2.9 ± 0.4 |
| Lungs | 0.9 ± 0.0 | 0.6 ± 0.0 | 0.9 ± 0.3 |
| Muscle | 0.3 ± 0.0 | 0.3 ± 0.0 | 0.4 ± 0.1 |
| Pancreas | 0.7 ± 0.0 | 0.7 ± 0.1 | 0.8 ± 0.1 |
| Spleen | 0.6 ± 0.0 | 0.6 ± 0.0 | 0.5 ± 0.1 |
| Testes | 0.1 ± 0.0 | 0.1 ± 0.0 | 0.1 ± 0.0 |

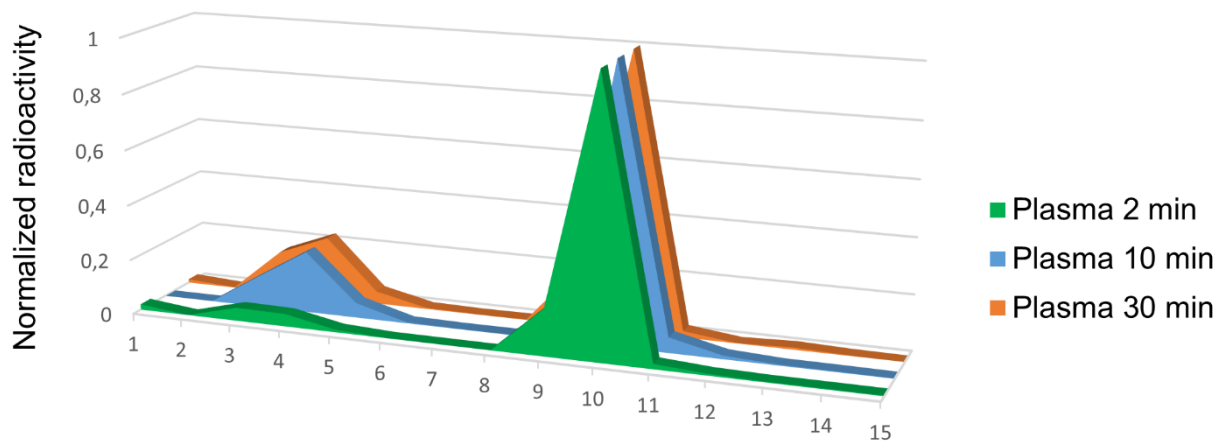
^a Percentage of injected dose calculated as (cpm in organ/total cpm recovered) x 100. ^b SUV calculated as (radioactivity in cpm in organ/weight of organ in grams)/(total cpm recovered/body weight). Data expressed as mean ± SD; n = 2 (control) or 3 (NMS-E973 and PU-H71) per time point.

Table S5: Biodistribution data of [¹¹C]NMS-E973 in B16.F10 melanoma inoculated C57BL/6 mice at 60 min after tracer injection with pretreatment of vehicle, PU-H71 or Ganetespiib.

| %ID ^a | | | |
|-------------------|----------------|---------------------|--------------------------|
| | 60 min control | PU-H71 pretreatment | Ganetespiib pretreatment |
| Blood | 2.6 ± 0.7 | 0.6 ± 0.2 | 0.6 ± 0.3 |
| Bone | 2.1 ± 0.0 | 0.8 ± 0.3 | 0.7 ± 0.6 |
| Brain | 0.0 ± 0.0 | 0.0 ± 0.0 | 0.0 ± 0.0 |
| Carcass | 15.2 ± 0.5 | 9.2 ± 5.3 | 14.5 ± 8.0 |
| Heart | 0.3 ± 0.1 | 0.2 ± 0.0 | 0.2 ± 0.0 |
| Intestines | 43.4 ± 2.0 | 53.9 ± 7.3 | 49.4 ± 4.4 |
| Kidneys | 1.8 ± 0.2 | 0.3 ± 0.1 | 1.2 ± 0.3 |
| Liver | 6.8 ± 2.0 | 8.6 ± 3.1 | 5.8 ± 2.4 |
| Lungs | 0.5 ± 0.0 | 0.2 ± 0.1 | 0.3 ± 0.1 |
| Muscle | 8.2 ± 1.2 | 5.1 ± 1.0 | 6.4 ± 1.4 |
| Pancreas | 0.5 ± 0.1 | 0.5 ± 0.2 | 0.3 ± 0.3 |
| Spleen | 0.2 ± 0.0 | 0.1 ± 0.0 | 0.1 ± 0.0 |
| Stomach | 1.0 ± 0.3 | 0.3 ± 0.2 | 0.3 ± 0.1 |
| Tumor | 0.8 ± 0.3 | 1.0 ± 0.4 | 1.2 ± 0.5 |
| Urine | 27.4 ± 3.5 | 28.9 ± 11.2 | 25.7 ± 7.4 |

| SUV ^b | | | |
|------------------|----------------|---------------------|--------------------------|
| | 60 min control | PU-H71 pretreatment | Ganetespiib pretreatment |
| Blood | 0.4 ± 0.1 | 0.1 ± 0.0 | 0.1 ± 0.0 |
| Bone | 0.2 ± 0.0 | 0.1 ± 0.0 | 0.1 ± 0.0 |
| Brain | 0.0 ± 0.0 | 0.0 ± 0.0 | 0.0 ± 0.0 |
| Heart | 0.6 ± 0.0 | 0.3 ± 0.1 | 0.4 ± 0.1 |
| Kidneys | 1.4 ± 0.1 | 0.2 ± 0.0 | 0.9 ± 0.2 |
| Liver | 1.4 ± 0.3 | 1.6 ± 0.4 | 1.3 ± 0.6 |
| Lungs | 0.6 ± 0.1 | 0.3 ± 0.1 | 0.3 ± 0.0 |
| Muscle | 0.2 ± 0.0 | 0.1 ± 0.0 | 0.2 ± 0.0 |
| Pancreas | 0.6 ± 0.1 | 0.6 ± 0.1 | 0.5 ± 0.2 |
| Spleen | 0.4 ± 0.0 | 0.2 ± 0.1 | 0.2 ± 0.0 |
| Tumour | 0.5 ± 0.1 | 0.2 ± 0.0 | 0.2 ± 0.0 |

^a Percentage of injected dose calculated as (cpm in organ/total cpm recovered) x 100. ^b SUV calculated as (radioactivity in cpm in organ/weight of organ in grams)/(total cpm recovered/body weight). Data expressed as mean ± SD; n = 3 per time point.



Collected HPLC fractions

Figure S8: RadioHPLC analysis of plasma samples (radiometabolite study). Polar radiometabolite fractions for respectively 2, 10 and 30 min account for $11 \pm 4\%$, $25 \pm 6\%$ and $28 \pm 8\%$ of total plasma activity.